

## Supporting Information Manuscript

### Synthesis of Patient-Specific Nanomaterials

University of Toronto, Rosebrugh Building, Room 407, 164 College Street, Toronto, Ontario M5S 3G9, Canada.

<sup>2</sup>College of Chemistry & Chemical Engineering, Chongqing University of Science & Technology, University Town, Shapingba District, Chongqing 4013s31, PR China.

<sup>3</sup>Terrence Donnelly Center for Cellular and Biomolecular Research, University of Toronto, 160 College St, Room 230, Toronto, ON, M5S 3E1, Canada.

<sup>4</sup>Department of Chemical Engineering, University of Toronto, 200 College Street, Toronto, Ontario, M5S 3E5, Canada.

<sup>5</sup>Department of Immunology, University of Toronto, Medical Sciences Building, Room 7308, 1 King's College Circle, Toronto, ON M5S 1A8, Canada.

<sup>6</sup>SPARC BioCentre, The Hospital for Sick Children, The Peter Gilgan Centre for Research & Learning, 686 Bay Street, 21<sup>st</sup> Floor Toronto, ON M5G 0A4 Canada.

<sup>7</sup>Department of Chemistry, University of Toronto, 80 St. George Street, Toronto, Ontario, M5S 3H6, Canada.

<sup>8</sup>Department of Materials Science and Engineering, University of Toronto, Wallberg Building, 184 College Street, Suite 140, Toronto, Ontario M5S 3E4, Canada.

\*Corresponding author: warren.chan@utoronto.ca.

Keywords: nanoparticles, protein corona, mass spectrometry, tunable organic nanostructures, patient-specific nanomaterials

## Table of Contents

Figure S1   Remaining gold species following dialysis and purification. ....	4
Figure S2   ICP and BCA assay determines the synthetic yield of protein nanoparticles. ....	5
Figure S3   Low Magnification Transmission Electron Microscopy Images of Reaction Scheme. ....	6
Figure S4   Hierarchically clustered heatmap of proteins comprising PNPs from different underlying nanoparticle surface chemistries. ....	7
Figure S5   Various statistical analyses demonstrate significant association among underlying nanoparticle surface chemistries and protein composition. ....	8
Figure S6   Hierarchically clustered heatmap of proteins comprising PNPs from different biological fluids. ....	9
Figure S7   Protein coated-gold and protein nanoparticles conjugated with NHS-functionalized small molecule dyes. ....	10
Figure S8   Different strategies to incorporate dyes into protein nanoparticles ....	11
Figure S9   Degradation of fluorescently conjugated PNPs by proteinase K ....	12
Figure S10   Bone marrow derived dendritic cell activation <i>in vitro</i> . ....	13
Figure S11   Liver biochemistry for toxicological analysis. ....	14
Figure S12   Inflammatory status of mice injected with protein nanoparticles. ....	15
Figure S13   Weight change measured over 28 days after primary and secondary injections. ....	16
Figure S14   Liver pathology study ....	17
Figure S15   Gating Strategy for Analyzing Expression levels of CD86 and CD69 on B (B220 <sup>+</sup> ) cells at day 28. ....	18
Figure S16   Expression levels of CD86 and CD69 on B (B220 <sup>+</sup> ) cells at day 28. ....	19
Figure S17   Characterization of protein adsorption to different nanoparticle surfaces and measurement of HRP activity. ....	20
Figure S18   Canonical centroid analysis to measure the significant differences between patient serum adsorption patterns on nanoparticle surfaces. ....	21
Supplementary Tables. ....	22
Table S1   Physicochemical characterization of the size and shape tunability of templates and their associated protein nanoparticle products. ....	22
Table S2   Physicochemical characterization of templates conjugated with different surface chemistries and biological fluids. ....	23
Materials and Methods. ....	26
Materials. ....	26
Preparation of Gold Nanoparticles. ....	28
Nanoparticle Surface Functionalization. ....	29
Serum Incubation and Excess Protein Purification. ....	29

<b>Cross-linking the Surface Bound Protein.....</b>	<b>30</b>
<b>Nanoparticle Etching and Dialysis.....</b>	<b>30</b>
<b>Personalized Nanoparticle Purification.....</b>	<b>31</b>
<b>Nanoparticle Physicochemical Characterization.....</b>	<b>31</b>
<b>Quantification of Gold throughout the Reaction and Following Purification.....</b>	<b>32</b>
<b>Surface Protein Removal and Purification from Nanoparticle Surface.....</b>	<b>32</b>
<b>Protein Precipitation and Cleanup.....</b>	<b>33</b>
<b>Protein Quantification Using Bicinchoninic Acid Assay.....</b>	<b>33</b>
<b>Liquid Chromatography Tandem Mass Spectrometry (LC-MS/MS) Trypsin Digest.....</b>	<b>34</b>
<b>LC-MS/MS Quantification of Proteins and Analysis.....</b>	<b>34</b>
<b>Proteomics-Statistics Analysis.....</b>	<b>35</b>
<b>Nanoparticle Fluorescence Conjugation.....</b>	<b>36</b>
<b>Degradation of Protein Nanoparticles.....</b>	<b>37</b>
<b>Analysis of Hemolytic Properties of PNPs.....</b>	<b>37</b>
<b>Qualitative Analysis of Total Complement Activation by Protein Nanoparticles.....</b>	<b>38</b>
<b><i>In vitro</i> immunogenicity study in bone marrow derived dendritic cells.....</b>	<b>39</b>
<b>Short Term Innate Immunogenicity and Toxicology.....</b>	<b>39</b>
<b>Assembly of Horseradish Peroxidase Loaded Protein Nanoparticles.....</b>	<b>41</b>
<b>Detection of HRP-Protein Nanoparticles <i>In Vivo</i>.....</b>	<b>42</b>
<b>Statistics.....</b>	<b>42</b>
<b>Supplementary Works Cited.....</b>	<b>42</b>

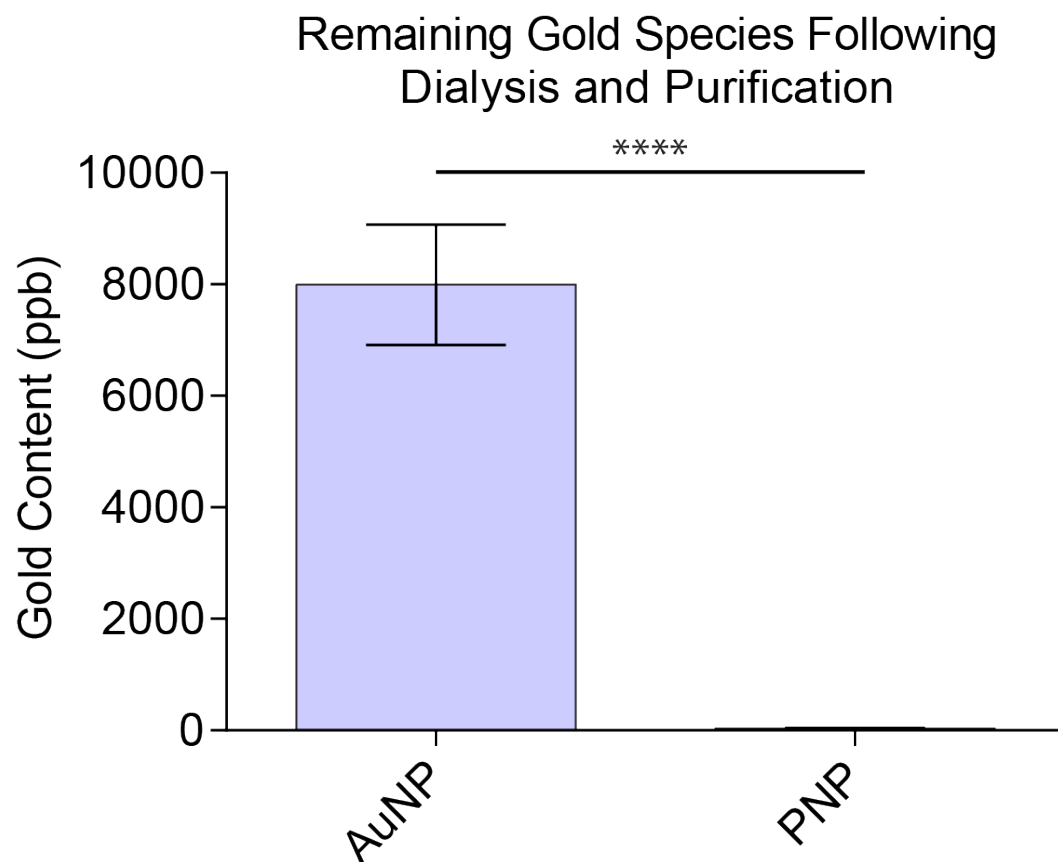


Figure S1 | **Remaining gold species following dialysis and purification.** 7993ppb gold was reacted to form protein nanoparticles. After etching and dialysis the protein nanoparticles retained only 35 ppb or 0.43% of initial gold content ( $P < 0.0001$ ). Error bars denote  $\pm$  standard deviation. Statistical significance was determined using an unpaired t-test with Welch's correction (\*\*\*\* $P < 0.0001$ ).

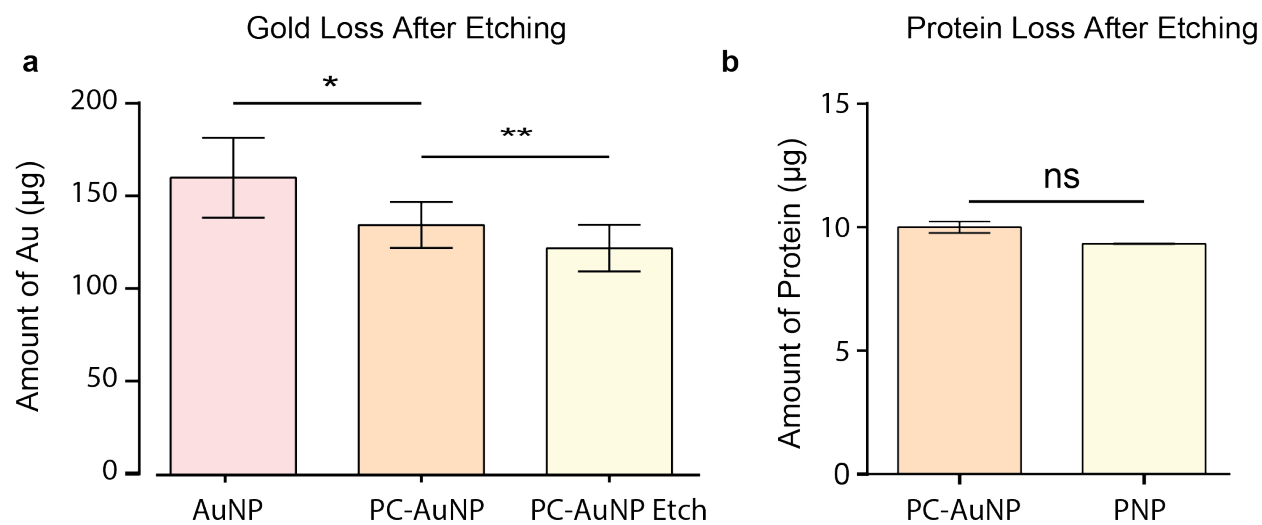


Figure S2 | **ICP and BCA assay determines the synthetic yield of protein nanoparticles.** PC-AuNP Etch is the direct measurement of the elemental gold signal and etchant following purification from the PNP. Error bars denote  $\pm$  standard deviation. Statistical significance was determined using an ANOVA and unpaired t-test with Welch's correction (\*\*\*\* $P < 0.0001$ ).

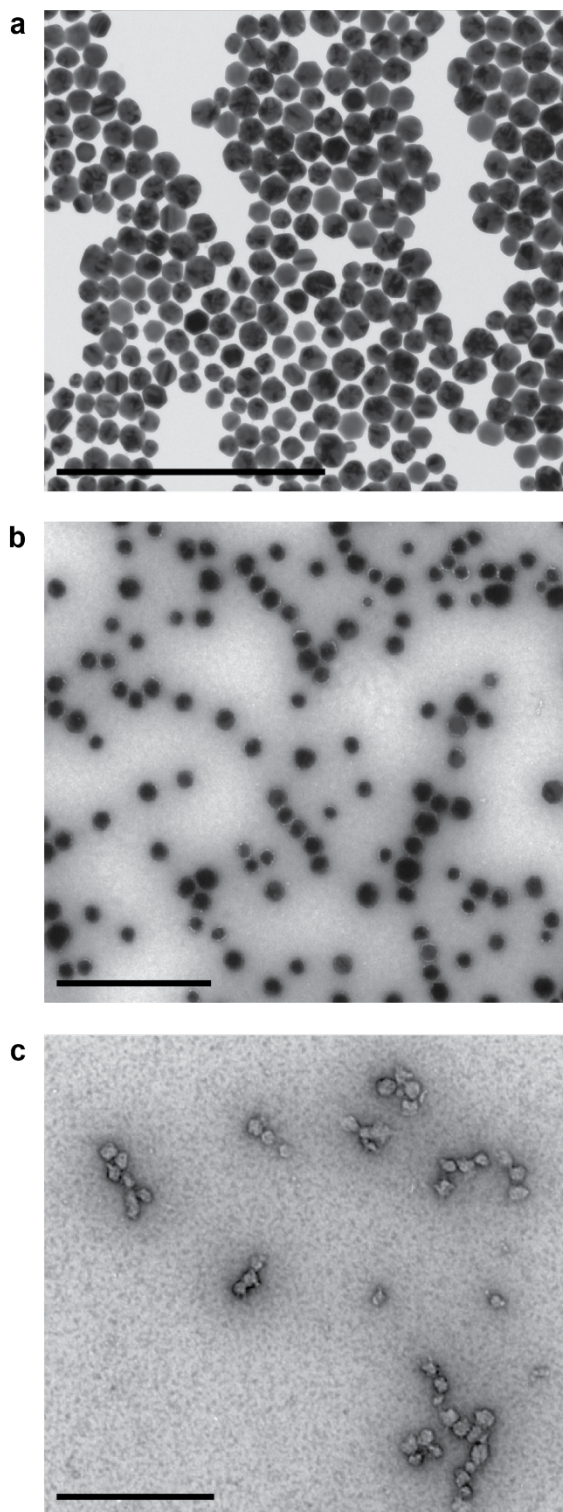


Figure S3 | **Low Magnification Transmission Electron Microscopy Images of Reaction Scheme.** We performed transmission electron microscopy on the entire synthetic workflow and show representative images of **a.** bare and **b.** protein-coated gold nanoparticles and **c.** protein nanoparticles. Scale bar, 100nm.

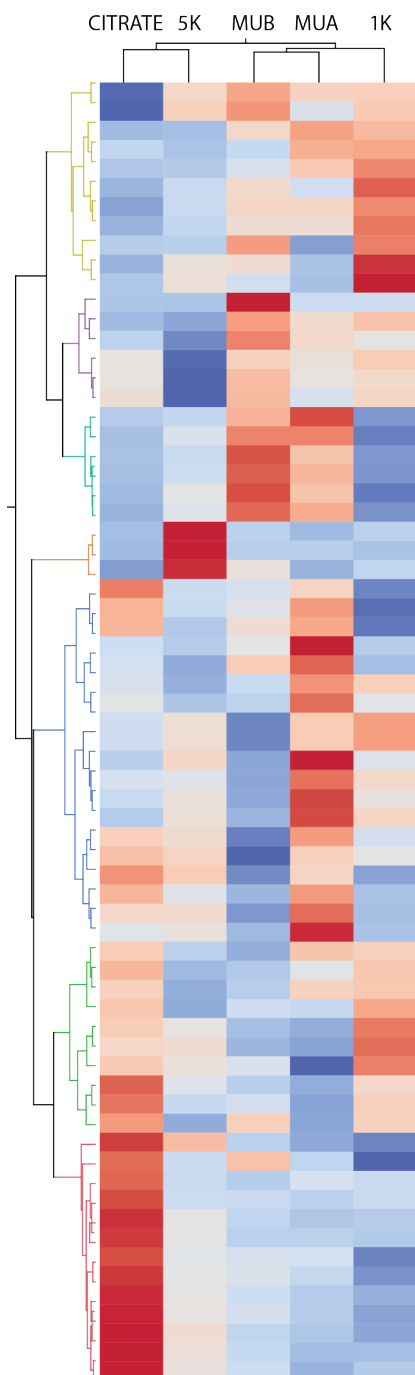
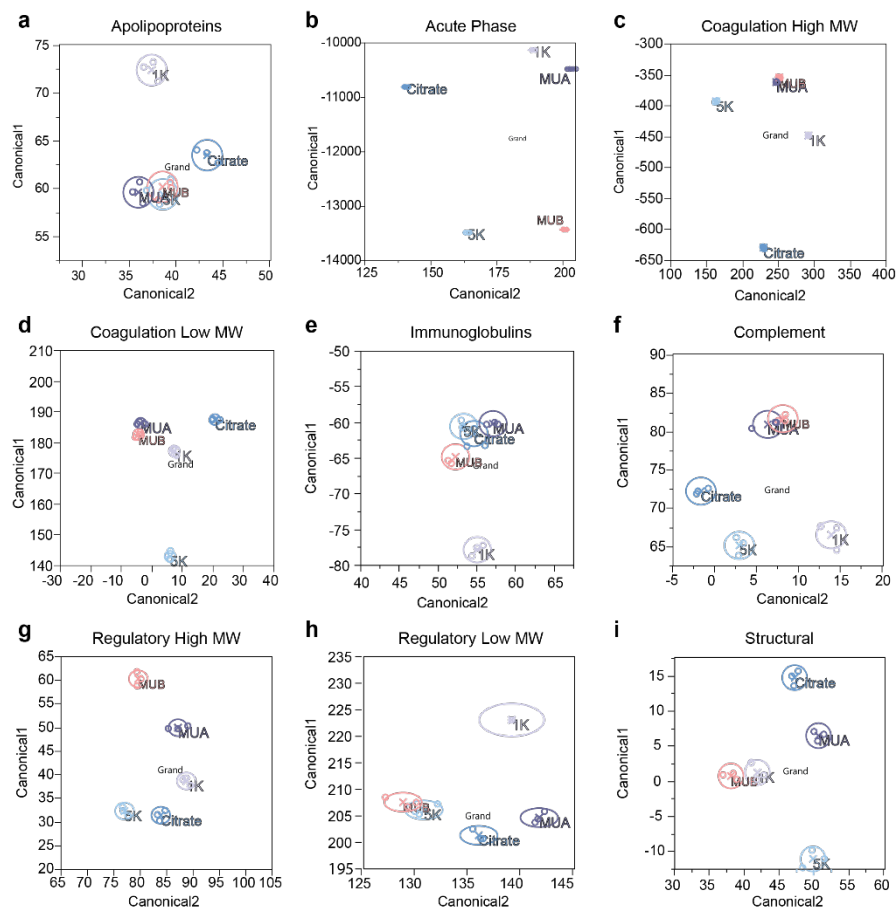


Figure S4 | **Hierarchically clustered heatmap of proteins comprising PNPs from different underlying nanoparticle surface chemistries.** Altering template surface chemistry to anionic, zwitterionic or cationic changes the distinct protein compositions found in PNPs. The hierarchically-clustered heatmaps show the most significant proteins (FDR P-value <0.05, test degrees of freedom = 4). The color represents the Z-score (red is above the mean and blue is below the mean of the  $\log_2$ -based label free quantitative protein abundance intensity). 1K, AuNP with 1 kDa polyethylene glycol. 5K, AuNP with 5 kDa polyethylene glycol. MUA, AuNP with mercaptoundecanoic acid.



**Figure S5 | Various statistical analyses demonstrate significant association among underlying nanoparticle surface chemistries and protein composition.** Conjugating nanoparticles with ligands that are anionic, zwitterionic or cationic enable the capture of different protein types from human serum to create different protein nanoparticles. **a.** Principal component analysis derived from mass spectrometry data shows the variability and statistically unique compositions derived from the different template surface chemistries. **b.** The statistically significant proteins that were discovered using the multivariable analysis of variance were classified according to their gene ontology function using the Universal Protein Resource. Associations were defined based on the generalized protein functional category. We performed a canonical centroid analysis to determine the variation in each composition and its significance in relation to all five conditions. The centroid for each condition is marked with an X and the colored circles represent the 95% confidence interval. After functional classification using the Universal Protein Resource, we find the significance between each class for **c.** apolipoproteins **d.** acute phase **e.** high molecular weight coagulation **f.** low molecular weight coagulation **g.** immunoglobulins **h.** complement **i.** high molecular weight regulatory **j.** low molecular weight regulatory **k.** structural proteins. Probability  $> F$  at least 0.0001 for each condition. 1K, gold nanoparticle with 1 kDa polyethylene glycol. 5K, gold nanoparticle with 5 kDa polyethylene glycol. MUA, gold nanoparticle with mercaptoundecanoic acid. MUB, gold nanoparticle with mercaptoundecyltrimethylammonium bromide, Citrate, gold nanoparticle with sodium citrate.



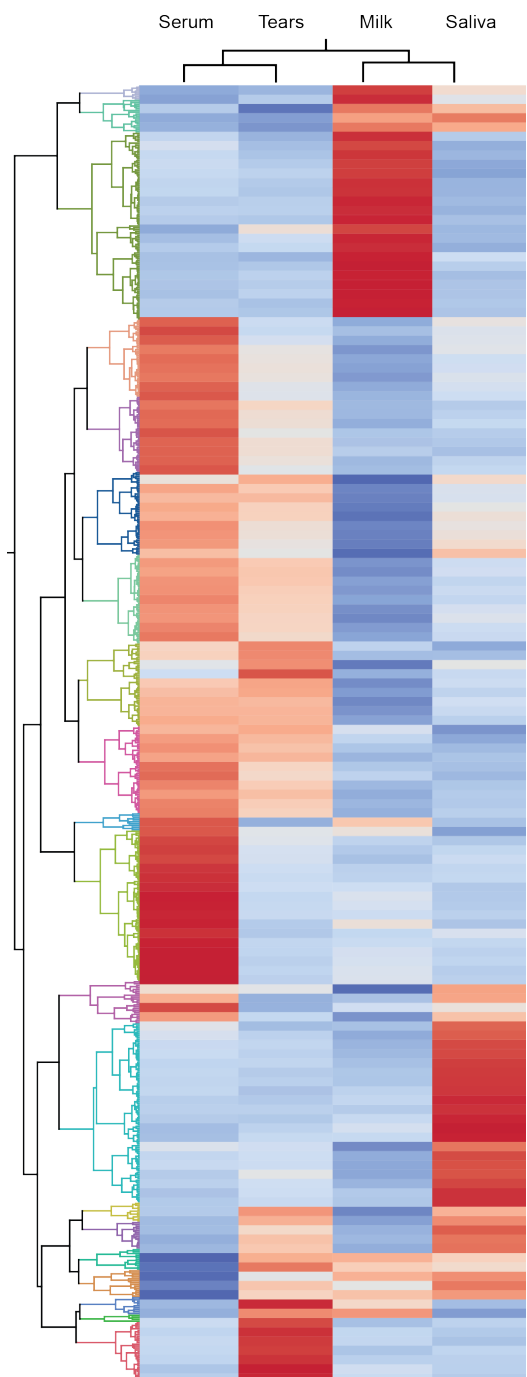


Figure S6 | **Hierarchically clustered heatmap of proteins comprising PNPs from different biological fluids.** **a.** Serum, breast milk, saliva and tears were isolated from patients, incubated with 50nm citrate-capped gold nanoparticle templates and used for protein nanoparticle (PNP) formation and proteomic analysis. Transmission electron microscopy images of **b.** tears **c.** serum **d.** milk and **e.** saliva demonstrate PNP formation. **f.** The heatmap shows the most significant proteins (FDR P-value <0.05, test degrees of freedom = 3) are clustered into twenty distinct groups. The color represents the Z-score, where red is above the mean and blue is below the mean of the  $\log_2$ -based label free quantitative protein abundance intensity.

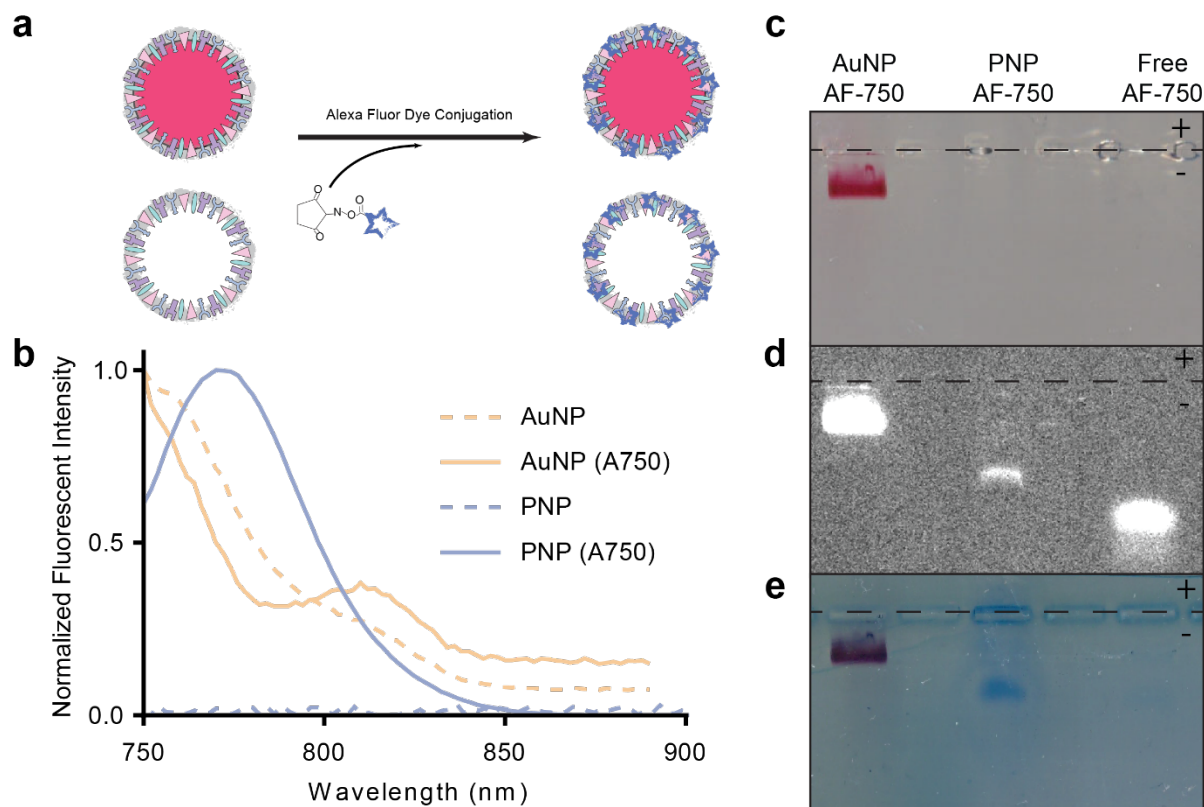
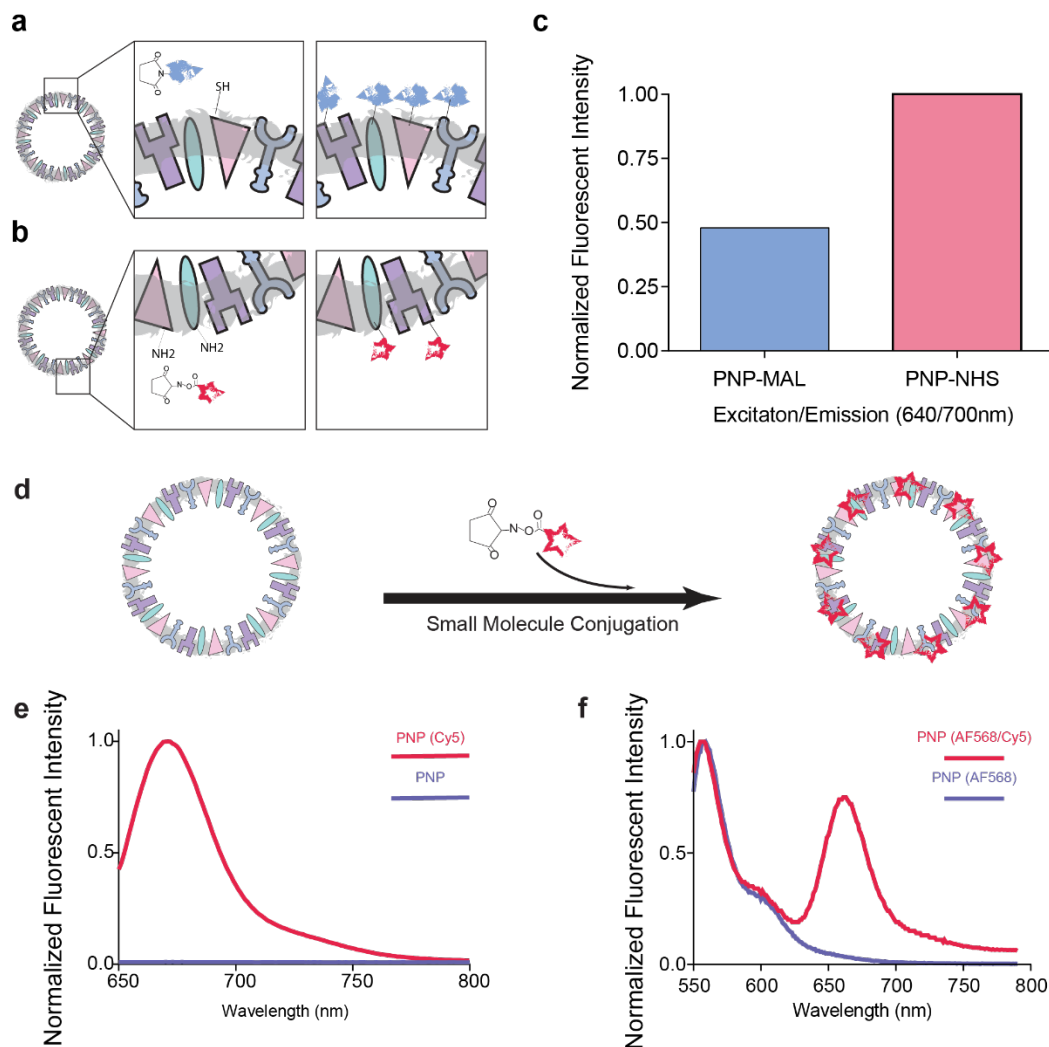
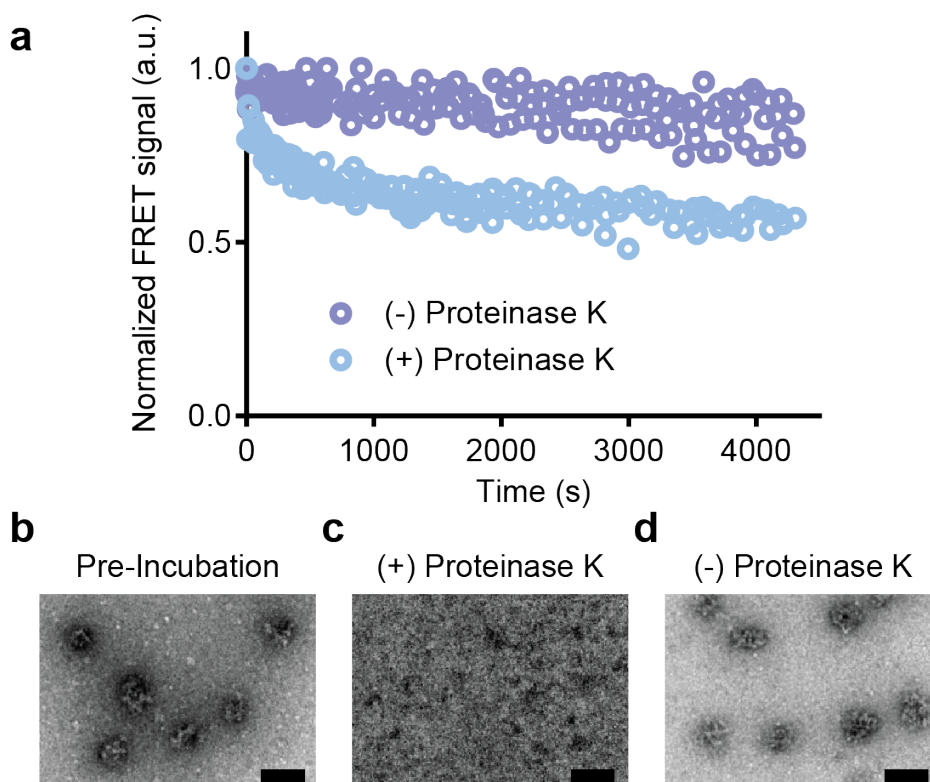


Figure S7 | **Protein coated-gold and protein nanoparticles conjugated with NHS-functionalized small molecule dyes.** **a.** The protein adsorbed and cross-linked onto the nanoparticle surface can be directly conjugated with a Cyanine-7 NHS-reactive small molecule dye. **b.** Fluorescent measurements using the FluoroMax-3 spectrofluorometer at an excitation wavelength of 750nm and emission at 830nm shows a positive fluorescent signal. **c.** A bright field image shows gold, **d.** fluorescent image shows the presence of dye and **e.** the location of protein that corresponds to the band found on the agarose gel.



**Figure S8 | Different strategies to incorporate dyes into protein nanoparticles** **a.** The protein adsorbed and cross-linked onto the nanoparticle surface can be directly conjugated with Cyanine-5-maleimide and **b.** Cyanine-5 N-Hydroxysuccinimide. **c.** Fluorescent measurements using the FluoroMax-3 spectrofluorometer at excitation and emission wavelengths of 640nm and 700nm respectively show the positive emission profiles of two different dyes with two different reaction chemistries. **d.** Alternatively, serum proteins can be conjugated with small molecules (Cyanine-5-N-Hydroxysuccinimide) prior to yield a simple and efficient strategy to form **d.** functional protein nanoparticles. **e.** Fluorescent measurements using a spectrofluorometer at an excitation wavelength of 630nm and emission at 700nm shows a positive fluorescent signal. **f.** Two different NHS-dyes, Cyanine-5 and Alexa Fluor-568 (Excitation 540nm, Emission range 550-800nm) were directly conjugated to the PNP surface. Based on the close excitation and emission bands between the two dyes, and their close proximity within the nanoparticle structure, they are capable of undergoing Förster resonance energy transfer.



**Figure S9 | Degradation of fluorescently conjugated PNPs by proteinase K.** **a.** PNPs were made with Cy5 and Cy3 conjugated human serum. The FRET ratio was followed over time in the presence or absence of proteinase K at room temperature. Traces are the average of three replicates. Representative TEM images were collected to show the morphology of PNP **b.** before incubation **c.** after exposure to Proteinase K and **d.** PBS. Scale bar, 100nm.

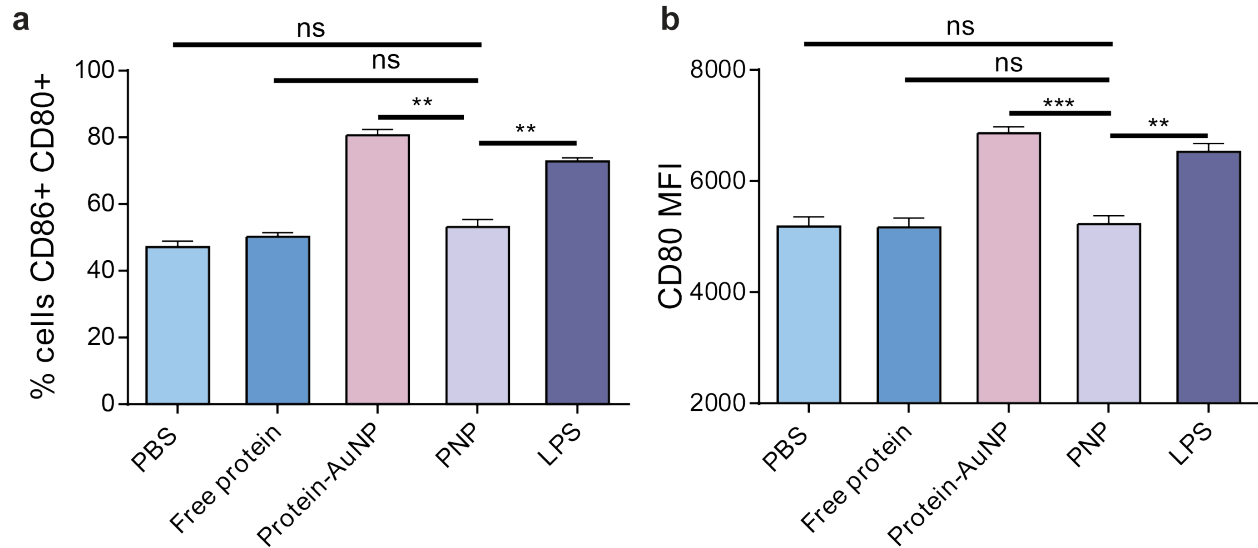


Figure S10 | **Bone marrow derived dendritic cell activation *in vitro*.** **a.** The percentage of dendritic cell expressing both CD86 and CD80 surface activation markers. **b.** Amount of activation markers of CD80 expressed on dendritic cell surface at day 2. No difference was found among PBS, free protein and PNP treated groups. Significantly higher dendritic cell activation was found in protein-AuNP and LPS than PNP group (\*\* $P > 0.01$  and \*\*\* $P > 0.001$  respectively.  $\pm$  denotes standard deviation ( $n=4$ ). Statistical significance was determined using one-way ANOVA with Tukey correction for multiple comparisons.

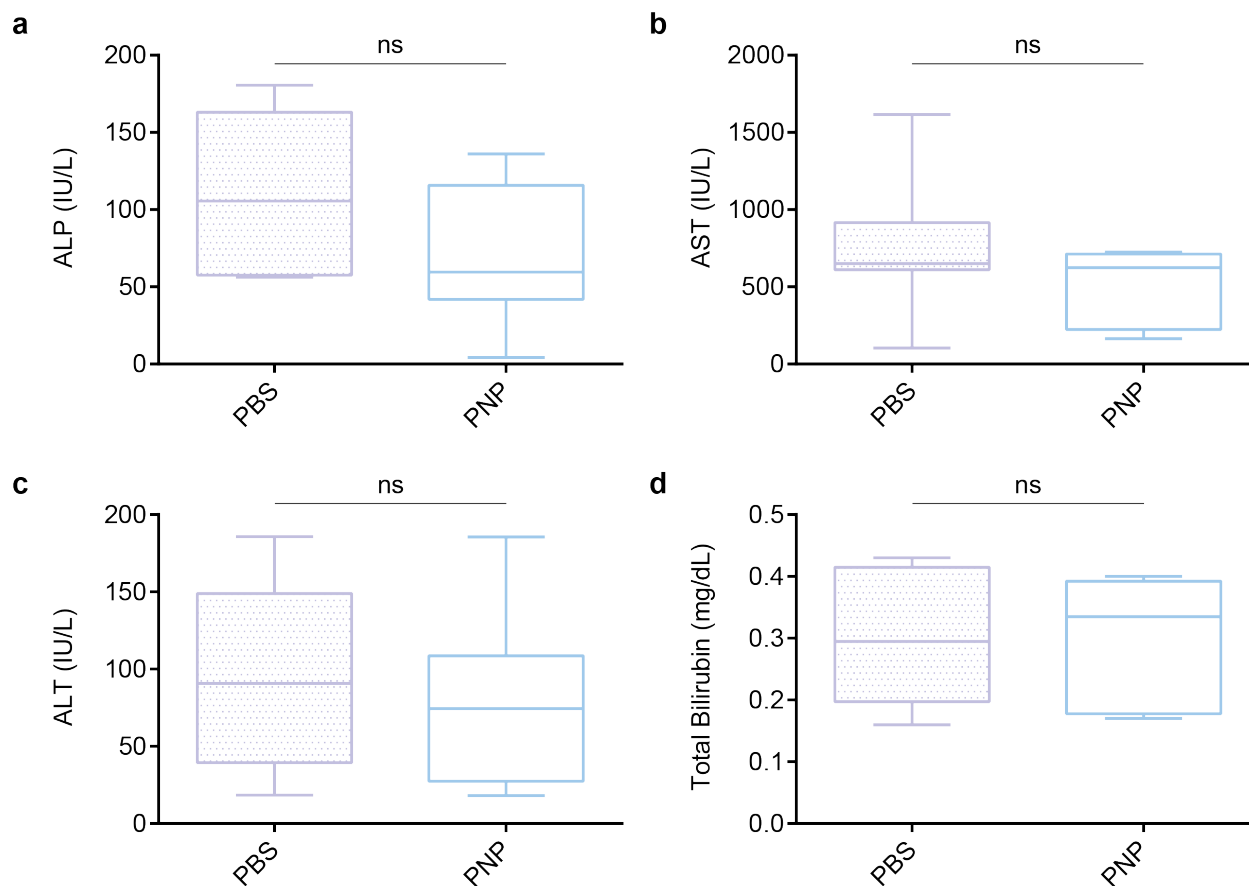


Figure S11 | **Liver biochemistry for toxicological analysis.** Blood was drawn from PBS and protein nanoparticle treated C57BL/6 mice to measure toxicity. Toxicity is determined by elevated markers of **a.** alkaline phosphatase **b.** aspartate aminotransferase **c.** alanine aminotransferase and **d.** total bilirubin. Significant hepatotoxicity was non-significant between vehicle and treated animals. Whiskers represent the 5<sup>th</sup>- 95<sup>th</sup> percentile from at least 7 independent replicates. There was no statistical difference between the treatment control and nanoparticle conditions as determined using an un-paired t-test with Welch's correction (ns=not significant).

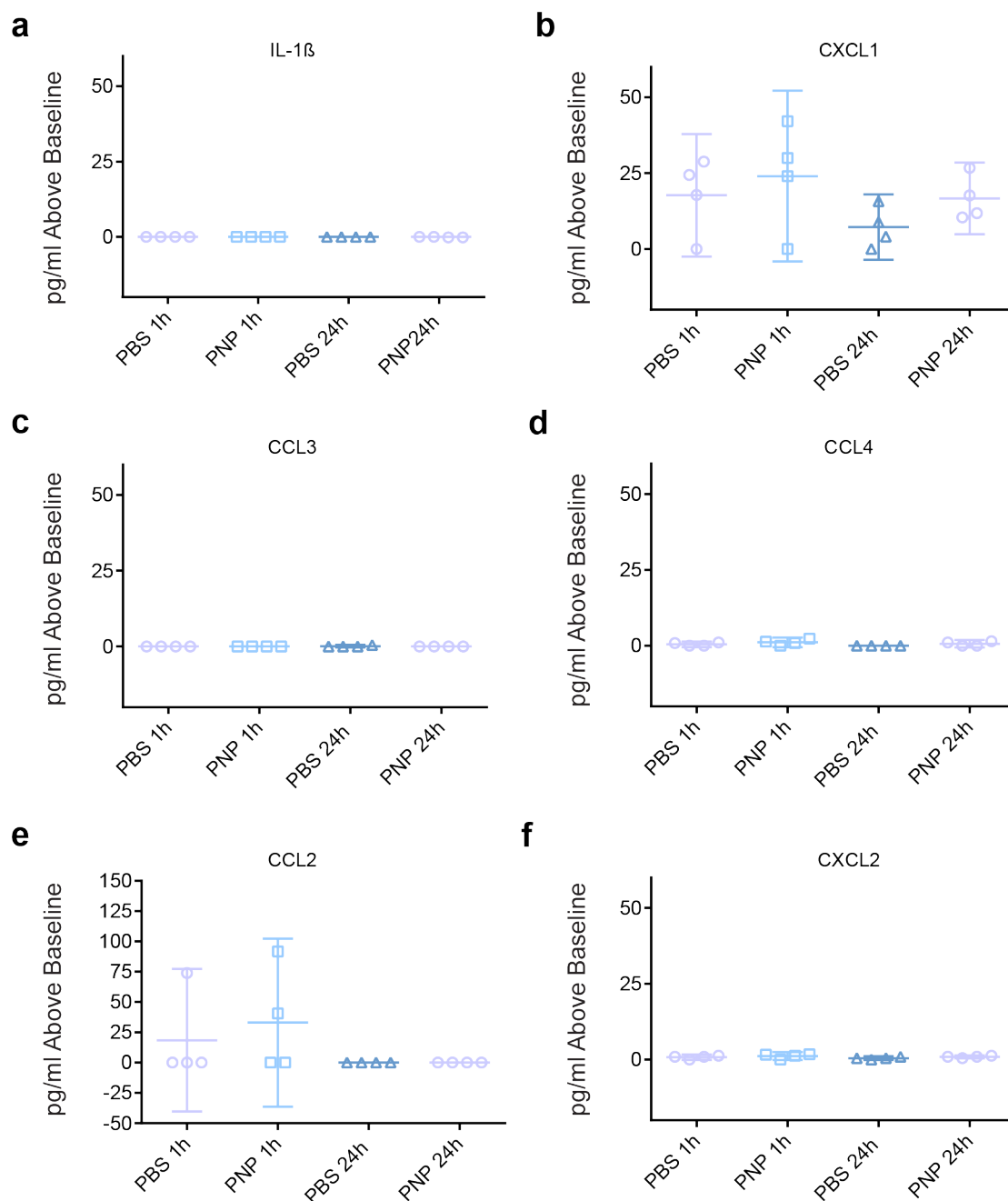
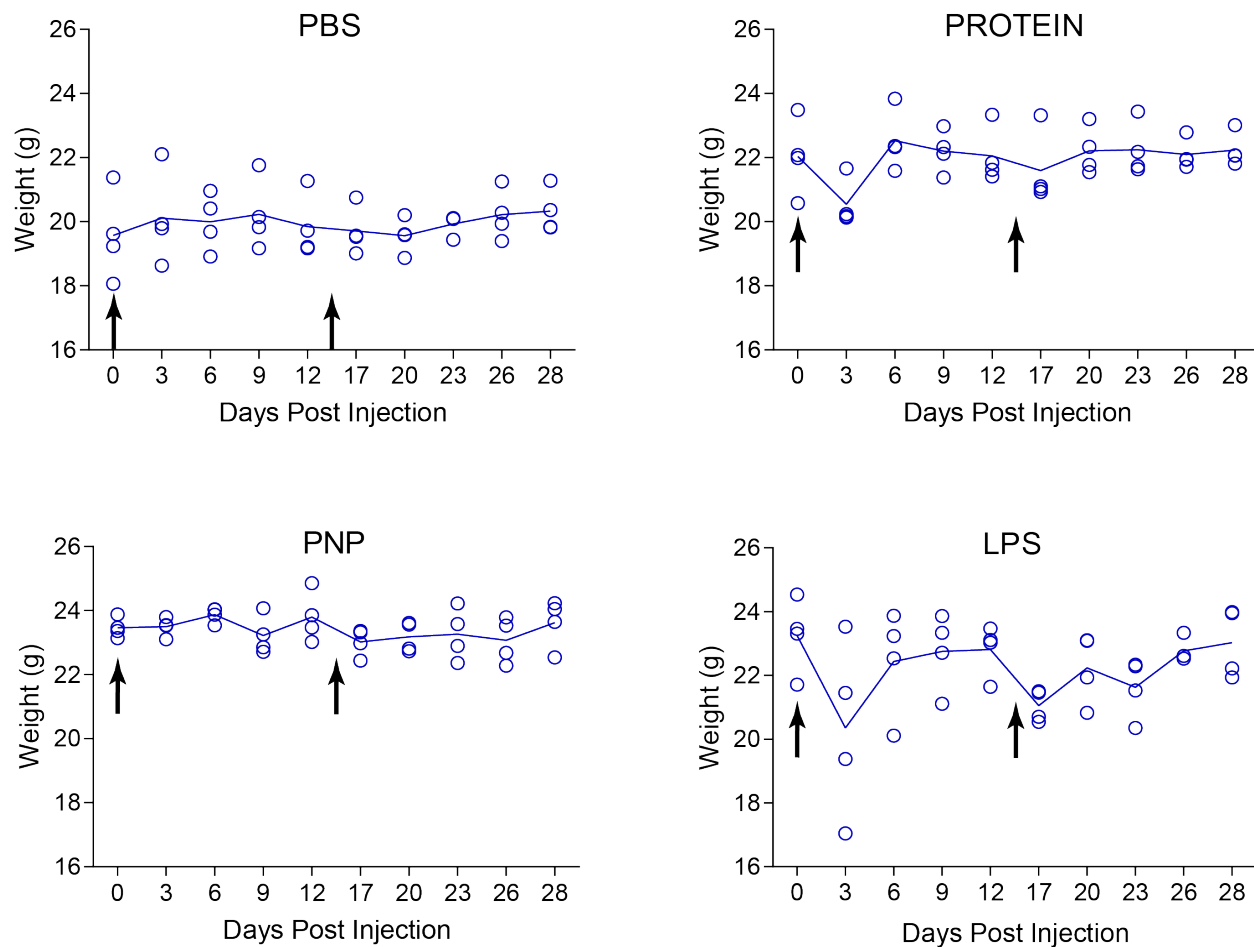


Figure S12 | **Inflammatory status of mice injected with protein nanoparticles.** Blood was drawn from PBS (vehicle) and protein nanoparticle treated (treated) C57BL/6 mice to measure concentration of indicated inflammatory mediators by Luminex assay. Each marker in panels a-f are known acute inflammatory markers of the innate immune system. Results showed no significant differences between vehicle and treated controls (n=4). Whiskers represent the 5<sup>th</sup>- 95<sup>th</sup> percentile from 4 independent replicates. Statistical significance was determined using one-way ANOVA. Zero values represent below threshold of detection for the assay.



**Figure S13 | Weight change measured over 28 days after primary and secondary injections.** No weight loss was found in PBS, protein and PNP groups, demonstrating mice are healthy after two injections of 50 mg/kg of protein or PNP vehicle. 20% body weight was lost after LPS primary and second injections. Black arrows indicate time of injection.



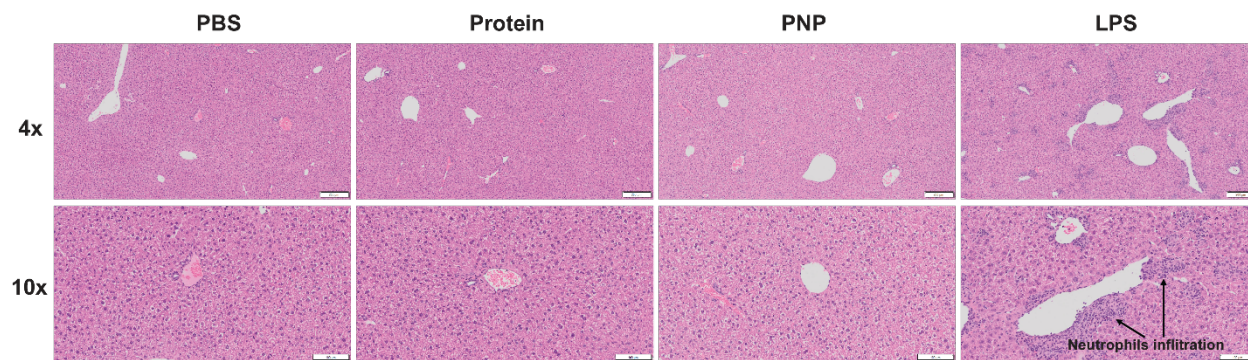


Figure S14 | **Liver pathology study.** No inflammation was observed in PBS, protein and PNP treated groups at day 28 after two times injections of 50 mg/kg. Severe inflammatory response (neutrophils infiltration) was observed in the LPS group.

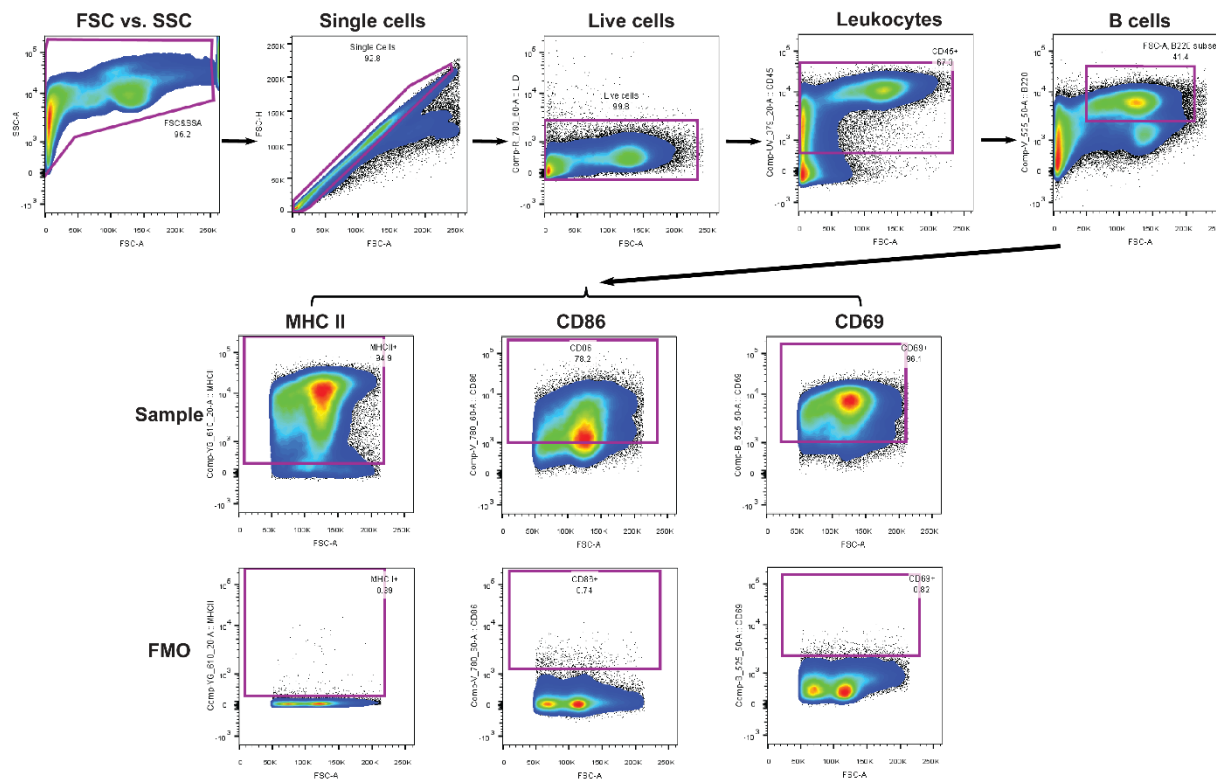


Figure S15 | Gating Strategy for Analyzing Expression levels of CD86 and CD69 on B (B220<sup>+</sup>) cells at day 28.

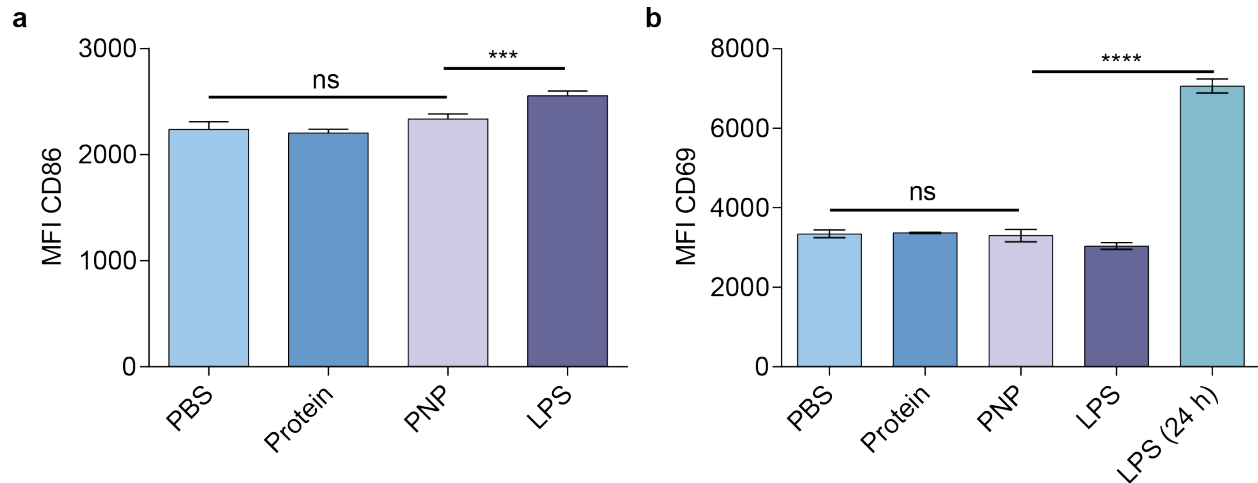
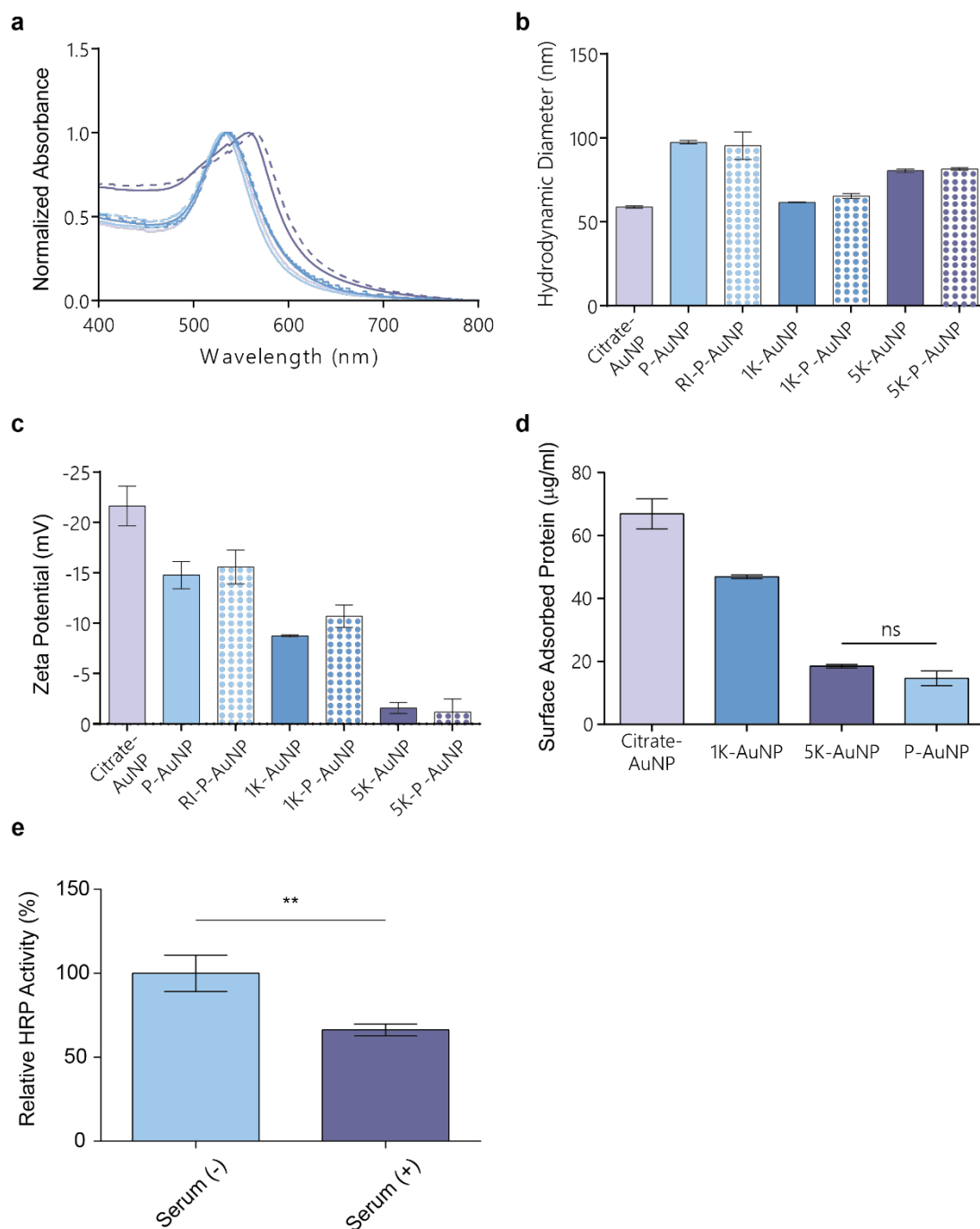
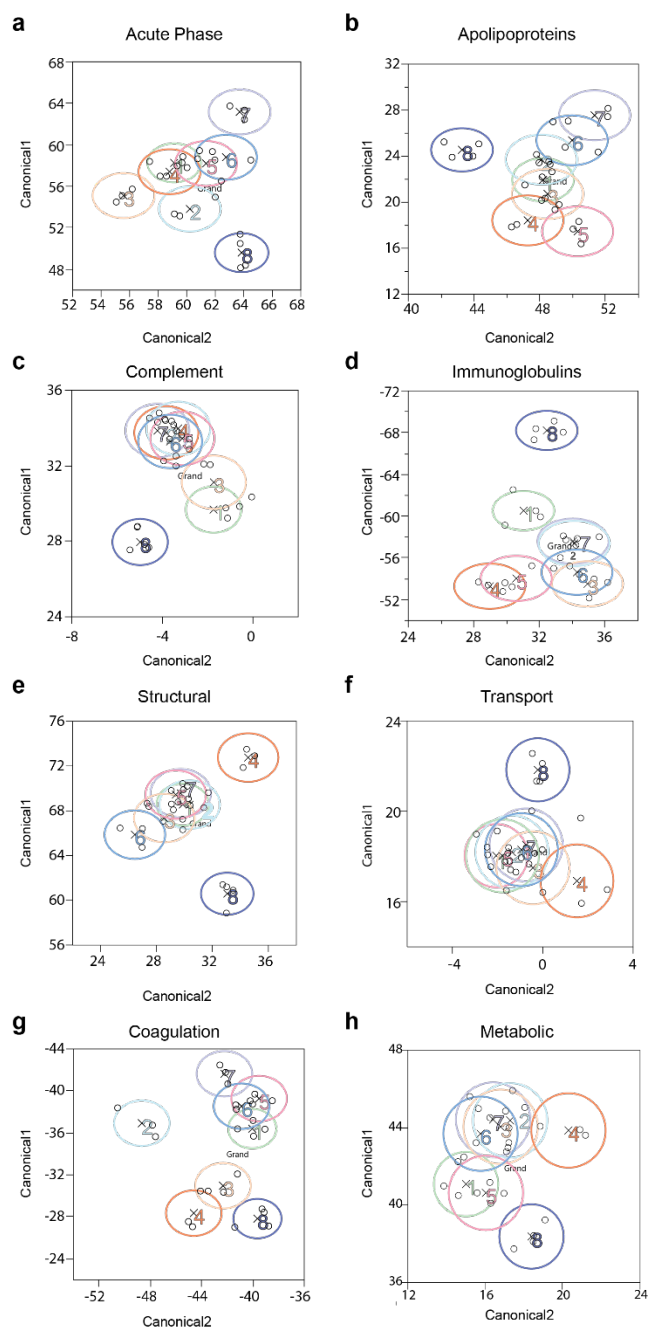


Figure S16 | **Expression levels of CD86 and CD69 on B (B220<sup>+</sup>) cells at day 28.** **a.** No difference was found among PBS, free protein and PNP treated groups. Significantly higher CD86 expression was found in the LPS treated group than PNP (\*\**P* < 0.001). **b.** A group of LPS treated at 24 hours was included for CD69 expression on B cell surface since CD69 is an early activated B cell marker. *In vivo* studies were *n* = 4 per condition. ± denotes standard deviation. Statistical significance was determined using one-way ANOVA with Tukey correction for multiple comparisons.



**Figure S17 | Characterization of protein adsorption to different nanoparticle surfaces and measurement of HRP activity.** 50 nm citrate-capped gold nanoparticles were either left unconjugated or bound at 5 molecules per square nanometer with one and five kilodalton polyethylene glycol. All nanoparticle surfaces including those coated in cross-linked protein were re-incubated (RI) with one hundred percent serum. We found that there was no change in **a.** surface plasmon resonance **b.** hydrodynamic diameter **c.** surface charge density and **d.** adsorbed protein on to the surface.  $\pm$  denotes standard deviation. Statistical significance was determined using an unpaired t-test with Welch's correction.



**Figure S18 | Canonical centroid analysis to measure the significant differences between patient serum adsorption patterns on nanoparticle surfaces.** We performed a canonical centroid analysis to determine the variation in each composition and its significance in relation to all five conditions. The centroid for each condition is marked with an X and the colored circles are the 95% confidence interval. After functional classification using the Universal Protein Resource, we find the significance among each class for **a.** acute phase **b.** apolipoproteins **c.** complement **d.** immunoglobulins **e.** structural **f.** transport **g.** coagulation and **h.** metabolic proteins. Probability > F at least 0.0001 for each condition.

## Supplementary Tables.

Template Type	Condition	Nanoparticle Core Size (nm)		Peak Plasmon Absorbance (nm)		Zeta Potential (mV)	Protein Quantity ( $\mu\text{g}/\text{cm}^2$ )
15 nm	AuNP	16.1 $\pm$ 1.2		522.2 $\pm$ 0.2		-18.0 $\pm$ 2.7	0.7 $\pm$ 0.1
	P-AuNP	25.3 $\pm$ 2.4		528.5 $\pm$ 0.6		-8.4 $\pm$ 0.7	
	PNP	31.0 $\pm$ 3.8		n/a		-4.5 $\pm$ 0.9	
30 nm	AuNP	28.8 $\pm$ 3.5		522.2 $\pm$ 0.2		-18.9 $\pm$ 1.5	2.2 $\pm$ 0.1
	P-AuNP	40.8 $\pm$ 3.1		528.6 $\pm$ 0.4		-13.2 $\pm$ 1.6	
	PNP	45.0 $\pm$ 2.3		n/a		-5.4 $\pm$ 1.8	
50 nm	AuNP	53.0 $\pm$ 4.4		530.3 $\pm$ 0.2		-22.6 $\pm$ 3.1	1.7 $\pm$ 0.2
	P-AuNP	66 $\pm$ 5.1		534.9 $\pm$ 0.2		-14.8 $\pm$ 1.2	
	PNP	69.3 $\pm$ 4.4		n/a		-7.6 $\pm$ 1	
30X10 nm	AuNP	32.5 $\pm$ 4.3	9.9 $\pm$ 2.0	508.5 $\pm$ 1.7	704.0 $\pm$ 1.4	17.3 $\pm$ 0.4	1.9 $\pm$ 0.1
	P-AuNP	39.4 $\pm$ 4.7	18.0 $\pm$ 2.8	509.0 $\pm$ 1.4	726.0 $\pm$ 2.0	-12.5 $\pm$ 1.5	
	PNP	39.8 $\pm$ 6.7	16.7 $\pm$ 5.1	n/a		-12.7 $\pm$ 0.3	

Table S1 | **Physicochemical characterization of the size and shape tunability of templates and their associated protein nanoparticle products.** Size measurements performed using transmission electron microscopy and diameter determined using ImageJ. All tests were performed with at least 3 technical and 3 biological replicates.  $\pm$  denotes standard deviation.

Surface ligand	Solvent/Biological Fluid	Hydrodynamic Diameter (nm)	PDI	Zeta potential (mV)	Peak absorbance (nm)
Citrate	0.05% Citrate	50	0.05	-19.0 ± 1.0	529 ± 0
1K PEG	0.05% Citrate	55	0.07	-14.0 ± 1.0	529 ± 0
5K PEG	0.05% Citrate	77	0.03	-2.3 ± 0.3	530 ± 0
MUA	0.05% Citrate	49	0.05	-26.5 ± 0.9	530 ± 0
MUB	0.05% Citrate	57	0.11	10.5 ± 0.5	530 ± 0
1K PEG	Human Serum	82	0.08	-15.0 ± 1.0	529 ± 0
5K PEG	Human Serum	77	0.03	-2.4 ± 0.5	530 ± 0
MUA	Human Serum	107	0.23	-13.6 ± 0.8	531 ± 0.6
MUB	Human Serum	107	0.24	-12.0 ± 2.0	534 ± 0
Citrate	Human Breast Milk	87	0.19	-17.0 ± 4.0	533 ± 0
Citrate	Human Tears	88	0.09	-12.6 ± 0.6	533 ± 0
Citrate	Human Saliva	89	0.16	-12.0 ± 1.0	530 ± 0.5

Table S2 | **Physicochemical characterization of templates conjugated with different surface chemistries and biological fluids.** All tests were performed with at least 3 technical and 3 biological replicates. ± denotes standard deviation. 1K, gold nanoparticle with 1 kilodalton polyethylene glycol. 5K, gold nanoparticle with 5 kilodalton polyethylene glycol. MUA, gold nanoparticle with mercaptoundecanoic acid. MUB, gold nanoparticle with mercaptoundecyltrimethylammonium bromide, Citrate, gold nanoparticle with sodium citrate.

<b>Protein Name</b>	
5'-nucleotidase	HLA (histocompatibility antigen) class I
Alkaline phosphatase, tissue- isozyme	HLA class I alpha chain E
Alkaline phosphatase, tissue- isozyme	HLA class I, B
Alpha-1-acid glycoprotein	HLA class I Cw-1 alpha chain
Alpha-1-antitrypsin	HLA class II, DP alpha 1 chain
Alpha-1-microglobulin	Hormonally up-regulated neu tumor-associated kinase
Alpha-2-antiplasmin	Ig kappa chain C region
Alpha-2-antiplasmin	Immunoglobulin J chain (IgA and IgM)
Alpha-2-antiplasmin	Immunoglobulin kappa
Alpha-2-HS-glycoprotein	Immunoglobulin lambda constant 7
Alpha-aminoadipic semialdehyde dehydrogenase	Immunoglobulin light chain, lambda gene cluster
Alpha-amylase	Insulin-like growth factor II
Antithrombin-III	Insulin-like growth factor-binding protein 3
Apolipoprotein A-I	Integrin alpha-M
Apolipoprotein B-100	Isocitrate dehydrogenase
Apolipoprotein(a)	Lactoferrin
Azurocidin	Lipoprotein lipase
Beta-2-glycoprotein 1 (Apolipoprotein H)	L-lactate dehydrogenase
Beta-2-microglobulin	Macrophage colony-stimulating factor 1
Carcinoembryonic antigen-related CAM 5	Matrix metalloproteinase-9
Ceruloplasmin	Monocyte differentiation antigen CD14
Coagulation factor IX	Monocyte differentiation antigen (Myo4)
Coagulation factor V	Mucin-1
Coagulation factor VII	Myeloperoxidase
Coagulation factor XI	Neutral alpha-glucosidase AB
Coagulation factor XII	Pancreatic alpha-amylase



Coagulation factor XIII A chain	Parathyroid hormone-related protein
Complement C1q subcomponent subunit A	Phospholipase A2
Complement C1s subcomponent	Plasma kallikrein
Complement C4	Plasma protease C1 inhibitor
Complement factor B	Plasminogen activator inhibitor 1
Complement Factor H	Platelet basic protein
C-reactive protein	Platelet glycoprotein 4
Creatine kinase U-type, mitochondrial	Platelet glycoprotein IX
Cystatin-C	Platelet-derived growth factor subunit B
Cysteine-rich C-terminal protein 1	Prolactin-inducible protein
Endoplasmic reticulum aminopeptidase 1	Calprotectin L1H
Ferritin	Prothrombin
Fibrillin-2	Prostate-specific membrane antigen-like protein
Fibrinogen alpha chain	Pyruvate kinase
Fibrinogen gamma chain	Retinol-binding protein 3
Fibronectin	Transferrin
Fructose-bisphosphate aldolase C	Serum albumin
Galectin-3-binding protein	Sex hormone-binding globulin

## Materials and Methods.

**Materials.** Aqueous gold (III) chloride (cat#S4641), Sodium citrate dibasic trihydrate (citrate) (cat#S4641), hydroquinone (cat# H17902), Tween20 (cat#[P2287](#)), hexadecyltrimethylammonium bromide (cat#H5882), mercaptoundecanoic acid (MUA) (cat#450561), tetramethylammonium hydroxide (TMAH) (cat#T7505), 97% sodium hydroxide (NaOH), (cat#221465), Mercaptoundecyltrimethylammonium bromide (MUB) (cat#733385), anhydrous reagent ethanol (cat#676829), Human serum (HS) (cat# H4522), rat serum (RS) (cat#R9759), goat serum (GS) (cat#G9023), rabbit serum (RAS) (cat#R9133), pooled mouse serum (MS) (cat#M5905), UltraPure™ glycine (cat#15527-013), sodium bicarbonate (bicarb) (cat# S6014) Potassium Iodide (cat#: P4286) (KI), Iodine (cat#: 38060) (I<sub>2</sub>), Agarose (cat#A9539), Yttrium standard for ICP (cat# 01357), trichloroacetic acid (TCA) (cat#T9159), acetone (cat#650501), sodium deoxycholic acid (DCA) (cat#30970), iodoacetamide (cat#I1149), porcine trypsin (cat#T6567), formic acid (FA) (cat#F0507), Bradford Reagent (cat#C57BL/6916-500ml), Anhydrous acetonitrile (ACN) 99.8% (cat# 271004), (cat#31216), Horseradish Peroxidase (HRP) (cat #P8375), SigmaFast OPD kit (cat# P9187), Hank's Buffered Salt Solution (cat # H6648), Trypsin-EDTA (cat# T4049), collagenase IV (cat#C5138), Drabkin's Reagent (cat#D5941), Brij® L23 solution (cat#B4184), bovine serum albumin (cat#9048-46-8), and EDTA (cat#6381-92-6) were all purchased from Sigma Aldrich. Cobra venom factor (cat# A2600) was purchased from Quidel. Veronal buffer saline (cat# IBB-250X) was purchased from Boston Bio Products. NHS-LC-sulfodiazarine cross-linker (cross-linker) (cat#PI2617), 100kDa Amicon tube (cat# UFC510096MI) and NuPAGE LDS buffer (cat#NP0008) were purchased from, Micro BCA Protein Assay Kit (cat# 23235), 2µm C18 beads (cat# ES800), Alexa Fluor 568 (cat#Z25006), Essential 8-Plex Mouse ProcartaPlex Panel 2 (cat# EPX080-20832-901), DNase I (cat# 90083), Proteinase K (cat#EO492), PageRuler Plus

Prestained Protein Ladder (cat#26619), Alexa Fluor™ 555 NHS Ester (cat#20009), goat anti-rabbit IgG Fc secondary antibody, Paraformaldehyde (cat#28908), 31-gauge insulin needle (cat#361041353), fetal bovine serum (cat#11875093), and IgG (Cat# 88-50400-86) and IgM (Cat# 88-50470-86) Uncoated ELISA Kit with Plates were all purchased from ThermoFisher Scientific. Anti-C3 antibody (cat#ab200999) was purchased from Abcam. Innovative grade C57BL/6 Mouse Serum recovered from normal healthy mice was purchased from Innovative Research, Novi, Michigan (cat#IGMS-BC-SER), Pooled human blood (Li-heparin)(cat#991-50-P), tears (cat#991-12-S), breast milk (cat#991-01-S), and saliva (cat#991-05-S) were purchased from Lee Biosolutions, Maryland Heights, Missouri, Patient sera (cat#PB007) was purchased from HemaCare, Van Nuys California, 0.22 µm polyethersulfone syringe (PES) filters (Millipore, cat#SLGP033RS), LoBind microcentrifuge tubes (Lobind tubes) (Eppendorf, cat#Z666505), TWEEN20 and DL-dithiothreitol (DTT) were purchased from BioShop, (cat#9005-64-5, cat#: DTT001.5), transmission electron microscopy copper grid (cat#01824G) were purchased from Ted Pella, Nitric (HNO<sub>3</sub>) and Hydrochloric acid (HCl) (Caledon Labs, cat#7525, cat#6025), Cyanine dyes were purchased from Lumiprobe (Cat# 43320), NAP-25 column (GE Healthcare, cat#: 17-0852-01), Tissue culture flasks T175 (112925) were purchased from Biomart, Toronto, Canada. Penicillin/streptomycin cocktail (Cat# 03-031-1B) was purchased from Biological Industries, Connecticut, U.S.A., ZipTip (EMD Millipore, Cat# ZTC18S09). 5kDa and kDa mPEG-SH (methoxy terminated-poly (ethylene glycol) MW: 1,5 kDa, Laysan Bio, Inc., Arab, AL (5K, 1K respectively). 4T1 (ATCC® CRL-2539™) cells were generously donated from Dr. Reginald Gorczynski, at University Health Network, University of Toronto, Canada. Anti-CD16/CD32, BUV395 and anti-CD45 (30-F11) were Purchased from BD-Bioscience. BV785 anti-CD11c (N418), PE/Dazzle594 anti-CD11b (M1/70), BV421 anti-CD86 (GL-1), FITC anti-CD80 (16-

10A1), Zombie NIR Live/Dead stain (Cat#423106), BV510 anti-CD45R/B220 (RA3-6B2), PE/Dazzle594 anti-I-A/I-E (M5/114.15.2), BV785 anti-CD86 (GL-1), FITC anti-CD69 (H1.2F3) were purchased from Biolegend. Granulocyte-macrophage colony-stimulating factor (GM-CSF) (cat# 130-095-746) was purchased from Miltenyi Biotec). RPMI media (cat#11875093) was purchased from Invitrogen. 1%P/S (Penicillin-Streptomycin solution) (cat#15140122) was purchased from Gibco. Flat bottom non-treated 24 Well culture plate (Cat#351147) was purchased from Falcon.

**Preparation of Gold Nanoparticles.** 15 nm gold nanoparticles were synthesized using the Frens gold-citrate reduction method<sup>[1]</sup>. Here, 0.25 mM gold chloride in 100ml of ultra-pure double distilled water (H<sub>2</sub>O) was brought to a rapid boil in a 250ml Erlenmeyer flask containing a 1.5” Teflon-coated magnetic stir bar. Citrate was added under rapid stirring speed to reduce the ionic gold solution, boiled for ten minutes to complete the reaction and placed in an ice bath. 30 and 50 nm AuNP were synthesized according to the Perrault and Chan method<sup>[2]</sup>. Briefly, 11.29 ml (30 nm) and 3.35 ml (50 nm) of 2.4 nM 15 nm AuNP were added to 100 ml of H<sub>2</sub>O under vigorous stirring in a 250 ml Erlenmeyer flask containing a 1.5” Teflon-coated magnetic stir bar. Then, 887  $\mu$ L (30 nm) and 967  $\mu$ L (50 nm) of 0.25 mM gold chloride and 887  $\mu$ L (30 nm) and 967  $\mu$ L (50 nm) of 15mM citrate were added. 887  $\mu$ L (30 nm) and 967  $\mu$ L (50 nm) of 25 mM of hydroquinone was added to start growth. The solution was stirred overnight and then stabilized with 0.05% v/v Tween20. Gold nanorods (AuNR) according to methods developed by the Murphy group and optimized by Hauck *et al*<sup>[3,4]</sup>. Following synthesis, the AuNP/AuNR solutions were purified to remove reactants by centrifugation at 13000g (rods) 7500g (15 nm), 3500g (35 nm) and 1800g (50 nm) and stored in the dark at 4°C until needed.

**Nanoparticle Surface Functionalization.** 40 cm<sup>2</sup> (or desired surface area) of AuNP were washed in 1 ml of 0.01% citrate, centrifuged at 1500g for 35 minutes at 4°C. For Pegylated AuNP, they were reacted with 10 mg/ml of 1K and 5K PEG at a density of 5PEG/nm<sup>2</sup> and incubated at 60°C for 1 hour. For MUA functionalization, AuNP were resuspended in 900 μL of H<sub>2</sub>O and added to 100 μL of 3 mM MUA in ethanol and incubated at 60°C for one hour. 10 μL of 300 mM TMAH in H<sub>2</sub>O was added after incubation to stabilize the AuNP. They were washed once in 3 mM TMAH to remove excess ligands, and then concentrated by centrifugation again (store in 1 mM NaOH). For MUB functionalization, AuNP were resuspended in 900 μL of H<sub>2</sub>O and added to 100 μL of 30 mM MUB in ethanol, and incubated at 60°C for one hour. AuNP were washed once in H<sub>2</sub>O to remove excess ligands, concentrated by centrifugation, and stored in 40 μL of H<sub>2</sub>O. All AuNP were stored at 4°C until use<sup>[5]</sup>.

**Serum Incubation and Excess Protein Purification.** The procedure to incubate nanoparticles with serum and subsequently purify remains the same for all protein sources. Human Serum (HS) was used to optimize the synthetic procedure and stored at -20°C until used. Rat (RS), goat (GS), rat albumin (RAS), and mouse sera (MS) were used for qualitative analysis. Isolated C57BL/6 serum, as well as human tears, breast milk, saliva and clinical patient sera were filtered with PES filters and aliquoted into Lobind tubes. Note, lobind tubes are critical in order to prevent nonspecific protein interactions and therefore prevent AuNP aggregation. All nanoparticle aliquots were added to the serum samples at a ratio of 10 μL of serum per cm<sup>2</sup> of nanoparticle surface. Similar to previous studies nanoparticles were serum incubated for 1h at 37°C<sup>[6]</sup> (this provides proteins the sufficient time to achieve thermodynamic and kinetic equilibrium)<sup>[7],[8]</sup>. In order to successfully coat AuNR in protein, they must next be cooled down to 4°C to precipitate the CTAB. Next, remove the precipitates with a 1000g spin and wash once more at 13 000g in

citrate. AuNP were centrifuged at the same speeds as previously reported, and washed twice in 750  $\mu$ L bicarb-Tween (0.05% v/v Tween20). Finally, AuNP with adsorbed protein were washed once with 1.2 ml of bicarb to remove excess tween and unbound protein. Once purified, nanoparticles were characterized using zeta potential, plasmon absorbance and size and morphological analysis. Prior to cross-linking, validate the total number of particles in solution.

**Cross-linking the Surface Bound Protein.** Immediately before use, prepare a 5 mg/ml stock of cross-linker in 0.1 M bicarb. Surface area changes relative to the nanoparticle core diameter, consequently cross-linker quantities were optimized to total surface area of nanoparticles in solution. Dilute cross-linker to  $1.37 \times 10^{17}$  cross-linker molecules/  $\text{cm}^2$ . Sonicate solution to ensure homogenous interactions between cross-linker and nanoparticles. Allow cross-linking to occur overnight at room temperature under rotation. The following morning, add 1 M Glycine to a final concentration of 35 mM to quench any unreacted cross-linker and return to rotator for a subsequent 15-30 minutes. Concentrate nanoparticles at previously mentioned speeds, remove supernatant, resuspend in 750  $\mu$ L with bicarb-Tween, sonicate and centrifuge again (repeat once afterwards). For the final wash, dilute in 750  $\mu$ L of bicarb. Sonicate prior to photoactivation. Take a 365 nm UV-light and photoactivate the diazarine group to yield a reactive triplet carbene that will bind with high affinity to any reactive amine group and form a stable covalent bond<sup>[9]</sup>. Prior to etching, validate the total number of particles in solution.

**Nanoparticle Etching and Dialysis.** A linear relationship exists between total gold content and quantity of iodine required for etching (data not shown). At high concentrations  $\text{AuI}_2^-$  can precipitate and damage protein structure. Furthermore, protein iodination occurs rapidly as some groups have higher affinity for Iodine than others. These coordination reactions occur mainly

through Van der Waals interactions and are therefore readily reversed when exposed to an aqueous environment during dialysis<sup>[10-12]</sup>. Freshly prepare a stock etching solution of 24:1 KI:I<sub>2</sub>. Dissolve 79.7 mg of KI in 950  $\mu$ L of H<sub>2</sub>O and add 50  $\mu$ L of 1.0 N solubilized I<sub>2</sub>. Vortex thoroughly. Resuspend nanoparticle aliquot to 50  $\mu$ L final volume and etchant according to:  $\text{Volume}_{\text{ETCHANT}} = (\text{Volume}_{\text{NP}}) * (\text{Surface Area}_{\text{NP}}) / 10 \text{ cm}^2$ . The concentrations of etchant may be changed to accommodate the volume of your dialysis chamber. Add etching solution to nanoparticles and sonicate on and off for 30 seconds, and then rotate for 30 minutes to four hours at room temperature. Transfer etched solution to dialysis chamber and dialyze in 1X PBS, replacing buffer as needed until all color disappears from solution (this may take anywhere from two to twenty-four hours depending on the amount synthesized).

**Personalized Nanoparticle Purification.** Retrieve samples from dialysis cups and transfer to Lobind tubes. Centrifuge at 12 000g for 15 minutes at 4 °C to remove any protein-gold aggregates. The aggregates form a hard pellet at the bottom, so the entire supernatant may be removed. Add samples to Amicon tubes, add 400  $\mu$ L of bicarb and wash twice at 8000g for 10 minutes. Once purified, measure zeta potential and determine size and morphology using TEM. PNP were ran on 0.7% Agarose gel at 135V for 15 minutes and stained for two hours with Bradford Reagent in order to ensure that PNP morphologies visualized on TEM were not artefacts. A confined, visible and blue band indicated the presence of a homogenous population of PNP.

**Nanoparticle Physicochemical Characterization.** The average diameter and morphology of each batch of AuNP cores was characterized by TEM. Copper-mesh grids were plasma treated using a glow discharge lamp to remove organic contaminants. To improve overall image quality, do a final wash in water to minimize the formation of salt crystals. 5  $\mu$ L (between 1-10 nM) of nanoparticle stock were drop-casted onto the TEM grid, subsequently blotted and then dried for five minutes.

Protein samples were negatively stained with 3  $\mu\text{L}$  of 1% uranyl acetate, blotted and then dried for one hour. All samples were visualized at 200 kV (Technai 20, FEI, Hillsboro, OR, USA) and imaged using an AMT 16000 camera. The average nanoparticle size was determined using ImageJ (NIH) on at least fifty nanoparticles. Gold nanoparticle size was also determined using dynamic light scattering (DLS) and surface plasmon resonance, via ultraviolet-visible (UV-vis) spectroscopy (UV-1601PC; Shimadzu, Kyoto, Japan). We used this wavelength for the Beer-Lambert law to determine nanoparticle concentration. Surface charge density was analyzed with the Zetasizer Nano-ZS (Malvern Instruments Ltd., Worcestershire, UK) and confirmed with agarose.

**Quantification of Gold throughout the Reaction and Following Purification.** Inductive Coupled Plasma Mass Spectroscopy (ICP-MS) (NexION; Perkin Elmer, Waltham, MA, USA) was used to quantify the amount of gold that remained following etching and dialysis. A water bath was heated to 70°C. 400  $\mu\text{L}$  of  $\text{HNO}_3$  spiked with 1  $\mu\text{g}/\text{mL}$  Yttrium was added to 10  $\text{cm}^2$  of gold nanoparticles in glass tissue culture tubes and heated for two hours for digestion. Afterwards, 100  $\mu\text{L}$  of  $\text{HCl}$  was added. The samples were cooled to room temperature and diluted to a final  $\text{HCl}$  concentration of 0.02%. Particulates were filtered using a 0.22  $\mu\text{m}$  PES filter. A gold standard was prepared to measure the concentration of gold. All values were obtained from three independent and three technical replicates. Statistical significance was determined using an unpaired t-test with Welch's correction.

**Surface Protein Removal and Purification from Nanoparticle Surface.** 8  $\mu\text{L}$  of 4% LDS buffer and 4  $\mu\text{L}$  of 500 mM aqueous DTT was added to the concentrated AuNP stock following the last washing step. Subsequently, samples were incubated for one hour at 70°C and then centrifuged at 18 000g for 15 minutes. The gold aggregates pellet to the bottom and the stripped protein remains



in the supernatant. Purified protein stocks can be stored at  $-80^{\circ}\text{C}$  for Bicinchoninic Acid (BCA) Assay or Liquid Chromatography Tandem Mass Spectrometry (LC-MS/MS).

**Protein Precipitation and Cleanup.** BCA assay or LC-MS/MS for protein precipitation and cleanup share the same first steps. In order to remove detergents (SDS) and reducing agents (DTT) from the protein isolates they were washed with 10% (w/v) TCA in acetone and incubated at  $-80^{\circ}\text{C}$  overnight. The isolates were centrifuged at 18 000g for 15 minutes at  $4^{\circ}\text{C}$  to pellet the protein. The supernatant was then discarded and the pellet was resuspended in 500  $\mu\text{L}$  of 0.03% (w/v) DCA and vortexed thoroughly. Afterwards, 100  $\mu\text{L}$  of 72% (w/v) TCA was added, vortexed again, and incubated on ice for 30 minutes to re-precipitate proteins. The precipitated protein samples were centrifuged to a pellet at 18 000g for 15 minutes at  $4^{\circ}\text{C}$  and the supernatant subsequently removed. 1ml of acetone previously chilled at  $-30^{\circ}\text{C}$  was added to the pellet, vortexed rapidly and incubated at  $-80^{\circ}\text{C}$  for 1 hour. The precipitated protein samples were centrifuged to a pellet at 18 000g for 15 minutes at  $4^{\circ}\text{C}$ , supernatant subsequently removed. The purified protein pellet was air-dried for 1 hour and then stored at  $-80^{\circ}\text{C}$  until further use.

**Protein Quantification Using Bicinchoninic Acid Assay.** The purified protein pellet described previously was dissolved in 25  $\mu\text{L}$  of 2% (w/v) SDS dispersed in PBS. Standards of bovine serum albumin (BSA) were dissolved in a 2% (w/v) SDS solution dispersed in PBS. Both the standard and protein samples were incubated for one hour at  $70^{\circ}\text{C}$  to denature their primary structures. 200  $\mu\text{L}$  of BCA working reagent was added to the samples, standards and controls. They were then incubated for fifteen to thirty minutes at  $60^{\circ}\text{C}$  until an aquamarine color developed. The samples were cooled, transferred to a 96-well plate and absorbance measured using a Tecan Sunrise absorbance plate reader at 562 nm. The BSA standard was used to correlate absorbance to estimate total protein content in  $\mu\text{g}/\text{ml}$ .

**Liquid Chromatography Tandem Mass Spectrometry (LC-MS/MS) Trypsin Digest.** To reduce disulfide bonds in the protein pellets, 45  $\mu\text{L}$  of bicarb, 5  $\mu\text{L}$  of ACN, 5  $\mu\text{L}$  of 100 mM DTT (dissolved in bicarb) was added to each sample and incubated for one hour at 37°C. Then, the reduced disulfides were alkylated with 5  $\mu\text{L}$  of 500 mM iodoacetamide (in bicarb) and incubated for one hour at room temperature. Finally, to complete protein digestion 2  $\mu\text{g}$  of trypsin in 1mM HCl and incubated overnight at room temperature. 5  $\mu\text{L}$  of 20%w/v FA was added to decrease the pH and stop the reaction. The digested protein stocks were stored at -30°C until LC-MS/MS characterization (n=3 to 4 per condition).

**LC-MS/MS Quantification of Proteins and Analysis.** All species and patient samples were analyzed on a linear ion trap-Orbitrap hybrid analyzer equipped with a nanospray source and EASY-Nlc split-free nano-LC system (ThermoFisher, San Jose, CA). Zip Tips were used to desalt the digested protein stocks. Lyophilized peptides mixtures were then dissolved in 0.1% FA and loaded under pressure (600 BAR) onto a 75  $\mu\text{m}$ \*2 cm PepMap 100 Easy-Spray pre-column filled with 3 $\mu\text{m}$  C18 beads and subsequently an in-line 75  $\mu\text{m}$ \*50 cm PepMax RSLC EASY-spray column with 2  $\mu\text{m}$  C18 beads. Samples were eluted through a 0 to 35% ACN gradient in 0.1% FA for 60 minutes at a rate of 250 nL/min. Peptides were subsequently introduced into an LTQ-Orbitrap Elite hybrid mass spectrometer by nano electrospray. One MS full scan (400-1500 m/z) in the orbitrap analyzer was performed with an automatic gain control target of  $1 \times 10^6$ , a maximum ion injection of 120 ms, one microscan, and a resolution of 240,000. In the linear ion trap, ten data-dependent MS/MS scans were performed using the top ten most intense ions at 35% normalized collision energy in parallel with the MS scans.  $1 \times 10^5$  automatic gain control targets in MS/MS modes had a maximum injection time of 50ms, with MS/MS spectra triggered with a minimum ion intensity of 5000. Normalized collision energy was

set to 35 and a dynamic exclusion list of 500 and one repeat count occurred for 15 s and a repeat duration for 30 s. We used MaxQuant (v1.5.3.30) to process the raw MS files using standard workflow, and MS/MS spectra were searched against both mouse and human protein databases built into MaxQuant<sup>[13,14]</sup>. Protein LFQ represented the quantitative value of protein abundance, and were consequently normalized, missing values imputed and transformed into Z-scores using the Perseus software package (v1.5.2.6).

**Proteomics-Statistics Analysis.** LFQ values were normalized, and missing values were imputed using normal distribution default settings in Perseus software package (version 1.5.2.6). For each of the surface chemistry (SC), biological fluids (BF) and patient blood (PS) analyses, we obtained a list of 1266 corona proteins for which we had measurements of LFQ intensities. The data set contained either 3 or 4 biological replicates. We next performed ANOVA to screen responses for all 1266 proteins using the Response Screening platform of the JMP 12.2.0 (64 bit) software. In the ANOVAs, the factor surface chemistry (SC) was modeled as one nominal variable with 5 levels (1K, 5K, MUA, MUB, citrate); the factor biological fluids (BF) were modeled as one nominal variable with 4 levels (milk, tear, saliva, serum) and the factor patients (PS) was modeled as one nominal variable with 8 levels (Patients 1-8). Since the independent variable in the ANOVA was nominal, the software performed the regression with indicator variables. The Benjamini and Hochberg false discovery rate (FDR) threshold of 5% was used to select the proteins most likely to be affected by changes associated with the factor under study (either SC, BF or PS). This screening process resulted in sub-lists of protein of interest (FDR significant), composed specifically of 67 proteins for SC, 672 proteins for BF and 52 proteins for PS. Degrees of freedom ranged from 3-7 for all analyses.

For the SC and PS data, the list of FDR significant proteins was split into functional groups based on GO classification. The proteins in each of these functional groups were combined for MANOVA where the  $\text{Log}_2$  of the LFQ intensities of these proteins was used as the response dependent variable. The Fit Model platform of the JMP 12.2.0 (64 bit) software was used for this analysis with the regression “personality” selected as “MANOVA” and with “response specification” set to “identity”. This platform was also used to generate canonical centroid plots for each functional group of proteins.

The Multivariate Methods platform in JMP 12.2.0 was used for Principal Component Analysis of the FDR significant proteins in each data set (PS, BF or PS). The same platform was used to analyse the Z scores (defined across all levels of a specific factor, either SC, BF or PS) of all of the FDR significant proteins and to create heat maps and hierarchical clusters (Ward method). Two-way clustering was used to examine similarities between both different proteins and also different groups.

**Nanoparticle Fluorescence Conjugation.** Sulfo-Cy-5 and AF-568, AF-750, hydroxysuccinimide and Cy-5-maleimide were resuspended in 15  $\mu\text{L}$  of ACN and then diluted to 100  $\mu\text{L}$  with bicarb and reacted at a ratio of 10 000 dye/nanoparticle. For pre-conjugated serum, 100  $\mu\text{g}$  of dye was added to 500  $\mu\text{L}$  of serum. PNP were made as per the above protocol. Samples were covered in aluminum foil and rotated overnight and in the dark at room temperature. The following morning, nanoparticles were purified with a NAP-25 column, the run off collected, and then washed three times in Amicon filters in bicarb-Tween. The conjugation of dyes to protein was confirmed both by a spectrofluorometer (FluoroMax-3; Horiba, Kyoto, Japan), and agarose using the *In Vivo* imager (excitation/emission: 630/700nm) at 10 minutes exposure time. Maleimide dyes exhibit

lower fluorescent intensity because of lesser amounts of free thiol compared to free primary amines found in the protein.

**Degradation of Protein Nanoparticles.** 2 mL of HS was conjugated with 0.5 mg of Cy5-NHS or Cy3-NHS. The serum was incubated with dye at room temperature overnight. Dye-conjugated human serum was purified from excess dye using GE Healthcare illustra™ NAP™ Columns. 50 cm<sup>2</sup> of 50 nm AuNP was incubated with 85 μL of Cy5-conjugated HS and 85 μL of Cy3-conjugated HS (A total of 170 μL of dye-conjugated HS). PNPs were made as stated above, but protected from light wherever possible. After washing and purification, PNPs were diluted to 100 μL with 0.1 M pH 8 Hepes buffer. The fluorescence spectra of PNPs were recorded using a spectrofluorometer (FluoroMax-3, Horiba, Kyoto, Japan) (excitation/emission: 512/530-750 nm). A final concentration of 0.05% v/v of 20 mg/mL proteinase K or an equivalent volume of water was added to the PNPs (as a negative control). Three replicates of each condition were tested. The time of addition was recorded. Fluorescence spectra were recorded for 70 minutes. Subsequently, intensity<sub>cy5</sub>/intensity<sub>cy3</sub> was plotted against time. The morphologies of PNPs before and after degradation was also visualized using TEM.

**Analysis of Hemolytic Properties of PNPs.** The hemolytic assay was performed following a previously published protocol<sup>[15]</sup>. Briefly, pooled human blood was diluted with 1x PBS to give a total blood hemoglobin concentration of 10 g/L. PNPs were synthesized as stated above. Protein concentration of the PNPs was determined using a micro-BCA assay kit to create test concentrations that reflected our 250 mg/kg, 50 mg/kg, 10 mg/kg and 1 mg/kg injected dose *in vivo*. Hemoglobin calibration standards were made with concentrations: 0.8, 0.4, 0.2, 0.1, 0.05, and 0.025 mg/mL in Drabkin's reagent. A positive control of 1% Triton X-100 was used. The negative control was 1x PBS. 100 μL of test samples or controls were incubated with 700 μL of

1xPBS and 100  $\mu$ L of diluted blood in triplicate for 3 hours at 37°C. 100  $\mu$ L of test samples or controls were also incubated with 800  $\mu$ L of 1x PBS in triplicate for 3 hours at 37°C. After incubation, the samples were centrifuged for 15 minutes at 800xg. The supernatant was collected. 100  $\mu$ L of samples or 200  $\mu$ L of calibration standards was added per well in duplicate. 100 $\mu$ L of Drabkin's reagent was subsequently added to each well containing sample. Absorbance of the wells were recorded at 540 nm.

**Qualitative Analysis of Total Complement Activation by Protein Nanoparticles.** The western blot was performed following a previously published protocol<sup>[16]</sup>. Briefly, PNPs were synthesized as stated above. Protein concentration of the PNPs was determined using a micro-BCA assay kit to create test concentrations that reflected our 250 mg/kg, 50 mg/kg, 10 mg/kg and 1 mg/kg injected dose *in vivo*. Negative and positive controls of 1x PBS and cobra venom factor (with an activity of 50 U) respectively was used. Blood was collected by cardiac puncture and pooled from two C57BL/6 mice and anti-coagulated with K<sub>2</sub>EDTA. Plasma was collected from the blood by centrifugation for 10 minutes at 2500xg. 10  $\mu$ L of test samples or controls were mixed with 10 $\mu$ L of veronal buffer saline and 10  $\mu$ L of plasma in duplicate. Samples were incubated at 37°C for 30 minutes. Subsequently, 10  $\mu$ L of 4x NuPAGE buffer and 4  $\mu$ L of 500 mM DTT was added to the samples and heated to 95°C for 5 minutes. Samples were centrifuged at 21000g for 30 seconds, and supernatants were collected. 3  $\mu$ L of samples were loaded into a 10% polyacrylamide gel. PageRuler Plus Prestained Protein Ladder was loaded. Gels were ran at 100 V for 5 minutes, then 110 V for 60 minutes. Blots were transferred at 90 mA overnight. Membranes were incubated at 4°C in blocking buffer, then a 1/2000 dilution of rabbit anti-C3 antibody in blocking buffer overnight at 4°C. Membranes were washed twice, then incubated with a 1/10 000 dilution of AF-555 conjugated goat anti-rabbit IgG Fc secondary antibody in blocking buffer at room temperature

for 90 minutes. Membranes were washed twice, then imaged using an Carestream Multispectral MS Fx Pro In vivo imager (excitation/emission: 555/600 nm) with 10 minutes of exposure time.

***In vitro* immunogenicity study in bone marrow derived dendritic cells.** Tibia and femur was isolated from C57BL/6<sup>[17]</sup>. Bone marrow was collected from these bones and homogenized using a 10 ml syringe with 23-gauge needle in the petri dish. RPMI media with 10% de-activated FBS and 1% P/S was used to collect the bone marrow. 60-100 million bone marrow cells were collected from a mouse. 3 million cells were seeded into a non-treated 6-well plate in a total volume of 4 ml RPMI media with 20 ng/ml GM-CSF. Media was changed every 2 days. Bone marrow derived dendritic cells were collected on day 7 as loosely adherent cells. 200, 000 bone marrow derived dendritic cells/ well were seeded into a flat bottom non-treated 24 Well in 1 ml RPMI media. Negative PBS control, positive control LPS as well as free protein, protein coated AuNP and PNP (n =4) treated groups were used in this study. 50 ng/ml LPS was used as positive control for dendritic cell maturation.  $5^{10}$  particles were injected into each well. The injected protein amount was normalized based on the BCA quantification of PNP total protein amount. The treated dendritic cells were isolated after 48 hours and stained with antibodies for flow cytometry.

**Short Term Innate Immunogenicity and Toxicology.** 50 mg/kg of PNP were injected into 8-12 week old C57BL/6 mice purchased from Charles River Canada. They were then sacrificed one hour and one-day post-injection via cardiac puncture. The blood was isolated, and centrifuged down at 500g for 10 minutes. The serum was sent in two 50  $\mu$ L aliquots to the Toronto Centre for Phenogenomics for blood toxicology and the other for analysis of acute inflammatory markers. The serum was isolated and levels of IL-1 $\beta$ , CXCL1, CCL2, CXCL2 CCL3, and CCL4 were measured using a Luminex kit and the Magpix platform, as per the manufacturer's specifications.

Statistical analysis was performed using one-way ANOVA (\*\*P<0.01). All replicates represent different C57BL/6 mice subjected to the same treatment (n = 4-7).

**Sub-Acute Toxicology and Repeated Administration.** 16, 12-week old C57BL/6 mice were organized into four groups. The mice received two injections at day 0 and day 14. Group (1) received PBS only, group (2) 3 mg/kg of lipopolysaccharide, group (3) 50 mg/kg of free serum protein isolated from a C57BL/6 mouse and (4) 50 mg/kg of protein nanoparticles made from C57BL/6 serum. The mice were intravenously injected with a 31-gauge insulin needle into the tail vein. Mice behaviour was monitored daily, their weight recorded every three days and after the immune and booster shot their temperatures recorded (data not shown). After 28 days the mice were sacrificed and their blood removed via cardiac puncture. The blood was left to sit for 10 minutes at room temperature and then centrifuged at 500g for 10 minutes. The sera was diluted stepwise and IgG and IgM levels were recorded using Thermo Fisher Scientific quantitative ELISA kits according to manufacturer's protocols. Mice were watched daily for signs of stress. They were weighed every three days. After 28 days, the spleen was isolated and then mechanically disaggregated using a Razor blade and followed by enzyme disaggregation using 4790  $\mu$ L of HBSS buffer with 200  $\mu$ L of 10 mg/ml Collagenase IV and 10  $\mu$ L of 10 mg/ml of DNase in an Eppendorf. The Eppendorf was incubated at 37°C for 1 hour while rotating. Disaggregated splenocytes was then passed through a 70  $\mu$ L cell strainer and centrifuged at 300g for 10 mins at 4°C. After that, splenocytes were resuspended using HBSS and directly counted using a hemocytometer. Statistical analysis was performed using one-way ANOVA (\*\*P<0.01). All replicates represent different C57BL/6 mice subjected to the same treatment (n = 4). Liver pathology was studied by Immunohistochemistry. Liver section were fixed in 10% formalin for 1 day and sent to Toronto centre for phenogenomics for sample mounting and processing. The



sections were then stained with hematoxylin and eosin to reveal any gross inflammation. All animal handling, welfare, and protocols were approved by the Division of Comparative Medicine, University of Toronto, Canada.

**Antibody Staining and Flow Cytometry for Dendritic Cell and B-cell Analysis.** Cell suspension from bone marrow derived dendritic cell or splenocytes were stained with fluorescent labelled antibodies. Anti-CD16/CD32 antibody was used for Fc receptor blocking. Antibodies selected for dendritic cells are shown as follows, BUV395 anti-CD45 (30-F11)), BV785 anti-CD11c (N418), PE/Dazzle594 anti-CD11b (M1/70), BV421 anti-CD86 (GL-1), FITC anti-CD80 (16-10A1), Zombie NIR Live/Dead stain. Antibodies selected for B cell activation are shown below: BV510 anti-CD45R/B220 (RA3-6B2), PE/Dazzle594 anti-I-A/I-E (M5/114.15.2), BV785 anti-CD86 (GL-1), FITC anti-CD69 (H1.2F3). Cells were stained for 30 minutes on ice and followed by 2 washes using HBSS blocking buffer including 0.5% Bovine Serum Albumin and 2 mM EDTA. Cells were then fixed using 1.6% paraformaldehyde for 30 minutes on ice. Cells were finally resuspended in blocking buffer for flow cytometry. Cell stain events were acquired using a 5-laser BD LSRFORTESSA X-20 device. Events were analyzed using FlowJo V10 software and results were plotted and analyzed using Prism 6.0.

**Assembly of Horseradish Peroxidase Loaded Protein Nanoparticles.** Prepare HRP spiked HS stocks by making a 4 mg/ml solution of HRP. For 100%, 50%, 25%, 12.5% and 0%, to a final volume of 135  $\mu$ L with 10% HS. Prepare HRP-HS protein nanoparticles as per standard operating procedure. The procedure exhibits minimal functional activity when done with bicarb, but high activity in PBS. The purified nanoparticle's enzymatic activity was measured in the presence and absence of serum using the SigmaFast OPD kit. The relative turnover rate was determined based on the ratio of the absorbance value compared to the blank control. All values were obtained from

three independent and three technical replicates. Statistical significance was determined using an unpaired t-test with Welch's correction.

**Detection of HRP-Protein Nanoparticles *In Vivo*.** 50 mg/kg of HRP-protein nanoparticles and 50 mg/kg of free HRP were injected into 8-week old C57BL/6 mice who were then sacrificed one-hour post-injection via cardiac puncture. The liver was retrieved, weighed and cut into three pieces. First prepare the disaggregation solution which is 9.6 ml of HBSS, 400  $\mu$ L of 10 mg/ml collagenase and 10 mg of DNase I. The largest piece was first mechanically broken apart with scalpels and then placed in 5 ml of disaggregation solution for 30 minutes at 37°C. The solution was centrifuged for 10 minutes at 500g and then the supernatant (extracellular matrix and blood) was removed. 500  $\mu$ L of 0.1% Triton-X in H<sub>2</sub>O was added to lyse the purified cells. The liver cells, supernatant and other were added to the SigmaFast OPD kit. The relative turnover rate was normalized based on the volume and liver mass, and then compared to the ratio over the blank control. All values were obtained from two independent and three technical replicates. Statistical significance was determined using an unpaired t-test with Welch's correction.

**Statistics.** All statistics were performed using GraphPad Prism v6.01, and JMP statistical discovery software (V12.2.0) from SAS Institute Inc.

### Supplementary Works Cited

- [1] G. Frens, *Nature* **1973**, *241*, 20.
- [2] S. D. Perrault, W. C. W. Chan, *J. Am. Chem. Soc.* **2009**, *131*, 17042.
- [3] N. Jana, L. Gearheart, C. Murphy, *Chem. Mater.* **2001**, 2313.
- [4] T. S. Hauck, A. A. Ghazani, W. C. W. Chan, *Small* **2008**, *4*, 153.
- [5] C.D. Walkey, J. Olsen, F. Song, R. Liu, H. Guo, W. Olsen, Y. Cohen, A. Emili, W. C. W. Chan, *ACS Nano* **2014**, *8*, 2439.

- [6] C. D. Walkey, J. B. Olsen, H. Guo, A. Emili, W. C. W. Chan, *J. Am. Chem. Soc.* **2012**, *134*, 2139.
- [7] D. Dell'Orco, M. Lundqvist, C. Oslakovic, T. Cedervall, S. Linse, *PLoS One* **2010**, *5*, e10949.
- [8] S. Goy-López, J. Juárez, M. Alatorre-Meda, E. Casals, V. F. Puentes, P. Taboada, V. Mosquera, *Langmuir* **2012**, *28*, 9113.
- [9] A. F. Gomes, F. C. Gozzo, *J. Mass Spectrom.* **2010**, *45*, 892.
- [10] E. C. S. Transactions, T. E. Society, *ECS Trans.* **2012**, *41*, 53.
- [11] M. A. Wood, M. Riehle, C. D. W. Wilkinson, *Nanotechnology* **2002**, *13*, 605.
- [12] A. Davis, T. Tran, *Hydrometallurgy* **1991**, *26*, 163.
- [13] J. Cox, M. Mann, *Nat. Biotechnol.* **2008**, *26*, 1367.
- [14] J. Cox, M. Mann, *BMC Bioinformatics* **2012**, *13*, S12.
- [15] M. Dobrovolskaia, *Nanotechnol. Charact. Lab.* **2009**, *21702*, 1.
- [16] NCL Method ITA-5. **2010**, *21702*, 1.
- [17] K. Niikura, T. Matsunaga, T. Suzuki, S. Kobayashi, H. Yamaguchi, Y. Orba, A. Kawaguchi, H. Hasegawa, K. Kajino, T. Ninomiya, K. Ijro, H. Sawa, *ACS Nano* **2013**, *7*, 3926.